

IMPERIAL

Department of Mathematics

Deep Reinforcement Learning for Ad Personalization

Martin Batěk

CID: 00951537

Supervised by Mikko Pakkanen

2 September 2024

Submitted in partial fulfilment of the requirements for the
MSc in Machine Learning and Data Science of
Imperial College London

The work contained in this thesis is my own work unless otherwise stated.

Signed: Martin Batěk

Date: 17 July 2024

Abstract

ABSTRACT GOES HERE

Acknowledgements

ANY ACKNOWLEDGEMENTS GO HERE

Contents

1. Introduction	1
2. Background: Deep CTR Prediction	4
2.1. Problem Formulation and Ad Marketplace Data	4
2.2. Shallow CTR Models	6
2.2.1. Logistic Regression	6
2.2.2. Factorization Machines	7
2.3. Introducing MLPs in CTR prediction	8
2.4. Single vs Dual Tower Architectures	9
2.5. DNN Enhanced CTR models	10
2.5.1. Factorization-machine Supported Neural Networks	10
2.5.2. Wide and Deep	12
2.5.3. DeepFM	14
2.6. Feature Interaction Operator Models	15
2.6.1. Product Operators models	16
2.6.2. Convolutional Operator Models	20
2.6.3. Attention Operator Models	22
3. Background: Deep Reinforcement Learning	24
3.1. RL Basics: MDPs and Bellman Optimality Equations	24
3.2. Q-Learning and Deep Q-Learning	27
3.2.1. Q-Learning	27
3.2.2. Deep Q-Learning	28
3.3. DRN: Deep Reinforcement Learning for News Recommendation	29
4. Deep CTR model Evaluation	32
4.1. Models and Model selection Criteria	32
4.2. Experiment Setting	33
4.2.1. Datasets and Preprocessing	34
4.2.2. Evaluation Metrics	36
4.2.3. Optimization Algorithms	38
4.2.4. Hyperparameter Selection	38
4.3. Deep CTR Model Results and Discussion	39
4.3.1. Experiment 1: Comparative Model Analysis	39
4.3.2. Experiment 2: Hyperparameter Setting Analysis	42
5. Deep Reinforcement Learning for Ad Personalization	45
5.1. DRL-AP Algorithm	45

5.2. Experiment Setting	45
5.2.1. Simulating the Online Environment using KDD12	47
5.2.2. Evaluation Metrics	47
5.2.3. Hyperparameter Settings	48
5.3. Deep CTR-RL Results and Discussion	48
6. Conclusion	49
A. Appendix	A1
A.1. Abbreviations and Acronyms	A1
A.2. Notation	A1
A.3. Experiment Results	A1
A.3.1. Experiment 1: Comparative Model Analysis	A1

1. Introduction

The global digital advertising market is worth approximately \$602 billion today. Due to the increasing rate of online participation since the COVID-19 pandemic, this number has been rapidly increasing and is expected to reach \$871 billion by the end of 2027 (eMarketer, 2023). Many of the major Ad platforms such as Google, Facebook and Amazon operate on a cost-per-user-engagement pricing model, which usually means that advertisers get charged for every time a user clicks on an advertisement. This means that there is a significant commercial incentive to design Ad-serving platforms that ensure that the content shown to each user is as relevant as possible, so as to maximize user engagement and platform revenues as much as possible.

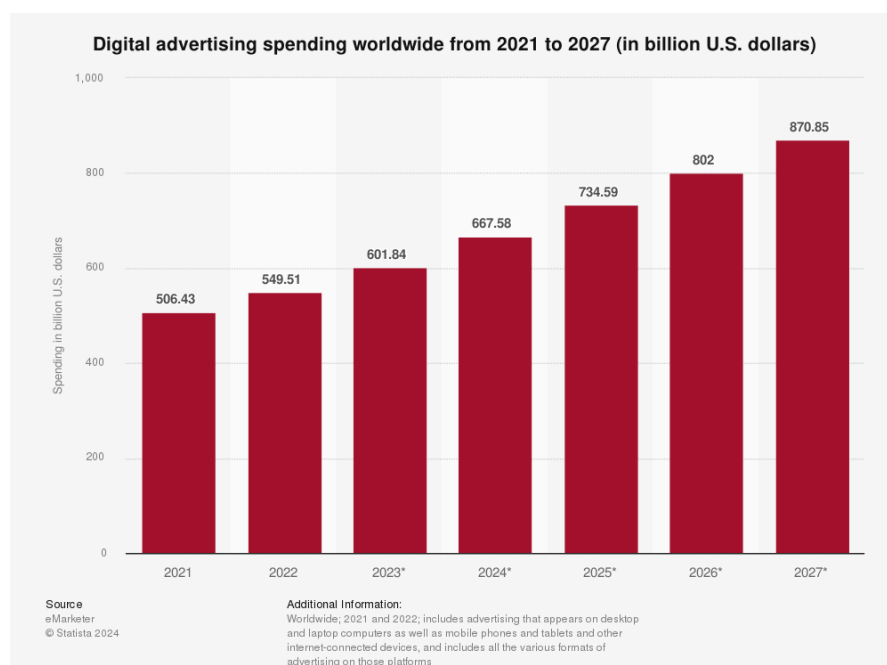


Figure 1.1.: Global Digital Ad Spending 2021-2027. Image taken from eMarketer (2023)

Attaining accurate Click-Through Rate (CTR) prediction is a necessary first step for Ad personalization, which is why study of CTR prediction methods have been an extremely active part of Machine Learning research over the past through years. Initially, shallow prediction methods such as Logistic Regression, Factorization Machines (Rendle, 2010) and Field-Aware Factorization Machines (Juan et al., 2016) have been used for CTR prediction. However, these methods have often been shown to be unable to capture

the higher order feature interactions in the sparse multi-value categorical Ad Marketplace datasets (Zhang et al., 2021). Since then, Deep Learning methods have been shown to show superior predictive ability on these datasets. A number of Deep Learning models have been proposed, each using a different techniques for feature interaction modelling, ranging from Deep Learning extensions of Factorization Machines such as DeepFM (Guo et al., 2017), to novel methods such as AutoInt (Song et al., 2019). By employing a multi-towered neural network architecture, these models are able to capture both low-order and high-order feature interactions in the data, and therefore tend to achieve superior predictive performance to their shallow counterparts.

However, irrespective of how well these models perform in a static environments, the reality is that user preferences and advertisement characteristics are constantly changing. Like most online recommender systems, Ad personalization models must be able to adapt to these changes in order to continue to provide accurate predictions over the longer period (Zheng et al., 2018). This problem necessitates the use of Reinforcement Learning for Ad personalization.

Reinforcement Learning is a subdomain of Machine Learning in which the goal is for an agent to learn an optimal policy that maximizes the expected reward in an environment where the state-action-reward progression can be modelled as a Markov Decision Process (Puterman, 2014). Early Reinforcement Learning methods involved deriving a the transition probabilities for the state-action pairs on the basis of interactions with the environment and then using Dynamic Programming methods such as the Upper Confidence Bound RL (UCB-RL) algorithm (Auer et al., 2008) and the the Thompson Sampling algorithm for Reinforcement Learning (Pike-Burke, 2024a). However, in cases where the state-action space is too sparse to be reasonably enumerated, it is often more practical to user a function approximator to directly estimate the expacted cumulative reward for each action in each state. This method of Reinforcement Learning is commonly referred to as Q-learning (Watkins, 1989), and has the advantage of being *model-free*, meaning that it does not require the agent to have a model of the environment thereby making it more scalable to large and sparse datasets. In (Hornik et al., 1989), (Cybenko, 1989) and (Hornik et al., 1990) Deep Neural Networks with activation functions are shown to be universal function approximators which naturally lead to the incorporation of DNN's in Q-Learning. This has lead to the development of the Deep Q-Learning Agent, which has been shown to be able to learn optimal policies in a number of different domains, such as the Atari 2600 game environment Mnih et al. (2015). Beyond this, Deep Reinforcement Learning has shown promising results in a number of different applications, including robot control and computer vision (Wang et al., 2024). In the context of Ad personalization, DRL has also be applied to online recommender systems such as News article recommendation (Zheng et al., 2018) and video recommendation on Youtube (Chen et al., 2019). In both papers, the authors show that the DRL agent is able to learn an optimal content recommendation policy on the basis of user engagement data. This reveals that there is potential for applying these methods to the problem of Ad personalization, thereby creating a truly adaptive marketing platform.

Research Question and Contributions

In this report, I aim to construct a Ad serving system that is truly adaptive and personalized to the changing user preferences and advertisement characteristics. In order to achieve this goal, I will first need to find a suitable Deep Learning Model architecture for CTR prediction, and then incorporating this model as the Q-function approximator in a Deep Q-Learning algorithm. The key contributions that I make in this report are as follows:

- I evaluate the performance of five popular Deep Learning models for CTR prediction on three well-known benchmark datasets, Criteo (Tien et al., 2014), KDD12 (Aden, 2012) and Avazu (Wang and Cukierski, 2014).
- I construct a novel Deep Reinforcement Learning Frame for Ad personalization, and as a proof-of-concept and evaluate its performance using the KDD12 dataset.

Structure of the Report

In chapter ??, I begin by providing a background introducing the problem of Click-Through Rate prediction in the context of Ad personalization, and explore the unique challenges posed by the typically sparse multi-value categorical datasets that are common in the Ad marketplace. I then proceed to review the literature on Deep Learning models for CTR prediction, highlighting the different techniques that each framework uses to capture the key feature interactions in the data. I also review the literature on Deep Reinforcement Learning, specifically the DRN algorithm introduced by Zheng et al. (2018), which can be analogously applied to the Ad personalization context. In chapter 4, I evaluate the performance of different Deep Learning models for CTR prediction on three well-known benchmark datasets, Criteo (Tien et al., 2014), KDD12 (Aden, 2012) and Avazu (Wang and Cukierski, 2014). In chapter 5, I construct a Deep Reinforcement Learning model for Ad personalization and evaluate its performance on the same benchmark datasets. Finally, in chapter ??, I discuss the results of the experiments and provide some concluding remarks.

2. Background: Deep CTR Prediction

2.1. Problem Formulation and Ad Marketplace Data

In their respective surveys on the use of Deep Learning methods for CTR prediction, Gu (2021) and Zhang et al. (2021) outline the problem of CTR prediction as one that essentially boils down to a binary (click/no-click) classification problem utilizing user/ad-view event level online session records. The goal of CTR prediction is to train a function f that takes in a set of ad marketplace features $\mathbf{x} \in \mathbb{R}^n$, and maps these to a probability that the user will click on the ad in that given context. In other words, $f_{\Theta} : \mathbb{R}^n \rightarrow \mathbb{R}$ such that:

$$\mathbb{P}(\text{click}|\mathbf{x}) = \mathbb{P}(y = 1|\mathbf{x}) = \sigma(f_{\Theta}(\mathbf{x})) = \hat{y} \quad (2.1)$$

where y is the binary click label, \hat{y} is the predicted likelihood that $y = 1$, Θ represents the parameter vector for f and $\sigma(x) = (1 + e^{-x})^{-1}$ is the sigmoid function. To ease the notation for the rest of the report, we will use the shorthand $p(y) = \mathbb{P}(y = 1|\mathbf{x})$ formulations in the following sections.

An instance of the ad marketplace features \mathbf{x} is typically recorded at a user/ad impression event level and typically consists of

- **User Features:** Features that describe the user, such as User ID, demographic information, metrics related to the user’s past interactions with the platform, etc.
- **Ad Features:** Features that describe the ad, such as Ad ID, Advertiser ID and Ad Category.
- **Contextual Features:** Features that describe the context in which the ad is being shown, such as the time of day, the position of the ad on the page and the site on which the ad is being shown.

Figure 2.1 shows a snapshot of the KDD12 dataset, which is a typical example of the type of data that is used for CTR prediction.

A defining characteristic for this type of data is that many of the features in \mathbf{x} are multi-value categories with a high degree of cardinality (He and Chua, 2017). In order to use categorical data in a classifier model, it is necessary to first convert the categorical values into suitable real valued vector representations. A common method for doing so is to encode these categorical features as *one-hot vector* representations. In other words, let feature x_i be a categorical feature with C_i distinct possible categories (i.e. with a *cardinality* of C_i). The one-hot vector representation of x_i then takes the form $\mathbf{x}_i^{OH} = (p_1, \dots, p_{C_i})$ where

Click	Impression	DisplayURL	AdID	AdvertiserID	Depth	Position	QueryID	KeywordID	TitleID	DescriptionID	UserID
0	1	4.29812E+18	7686695	385	3	3	1601	5521	7709	576	490234
0	1	4.86057E+18	21560664	37484	2	2	2255103	317	48989	44771	490234
0	1	9.70432E+18	21748480	36759	3	3	4532751	60721	685038	29681	490234
0	1	1.36776E+19	3517124	23778	3	1	1601	2155	1207	1422	490234
0	1	3.28476E+18	20758093	34535	1	1	4532751	77819	266618	222223	490234
0	1	1.01964E+19	21375650	36832	2	1	4688625	202465	457316	429545	490234
0	1	4.20308E+18	4427028	28647	3	1	4532751	720719	3402221	2663964	490234
0	1	4.20308E+18	4428493	28647	2	2	13171922	1493	11658	5668	490234
0	1	5.85475E+17	20945590	35083	2	1	35143	28111	151695	128782	490234
0	1	9.68455E+18	21406020	36943	2	2	4688625	202465	1172072	973354	490234
Target		Ad Features			User Features			Contextual Features			

Figure 2.1.: Snapshot of the KDD12 dataset Aden (2012)

$$p_k = \begin{cases} 1 & \text{if the value of } x_i \text{ is equal to the } k\text{-th possible category} \\ 0 & \text{otherwise} \end{cases}$$

The *sparse vector representation* $\tilde{\mathbf{x}}$ of feature vector \mathbf{x} is then given by the concatenation of one-hot vector representations of the categorical features $\{x_i\}_{i=1}^s$, and any real-valued features $\{x_i\}_{s+1}^{s+d}$:

$$\tilde{\mathbf{x}} = (\mathbf{x}_1^{OH}, \dots, \mathbf{x}_s^{OH}, x_{s+1}, \dots, x_{s+d}) \in \mathbb{R}^{\tilde{n}} \quad (2.2)$$

where s and d are the number of (sparse) categorical and (dense) numerical features in \mathbf{x} , and $\tilde{n} = \sum_{i=1}^s C_i + d$ is the size of $\tilde{\mathbf{x}}$.

The problem posed by high cardinality is that when C_i is large, most of the values in the sparse feature vector representation in equation 2.2 will be equal to zero for an overwhelming majority of observations. This can make it extremely difficult for a model to learn the key *implicit* features and patterns present in sparse data (Gu, 2021). An elementary method for alleviating this issue is to project the one-hot vector representations $\{\mathbf{x}_i^{OH}\}_{i=1}^s$ to some lower dimension $D < C_i \forall i \in [1, \dots, s]$. The *embedded* feature vector \mathbf{e}_i for categorical feature x_i is given by:

$$\begin{aligned} \mathbf{e}_i &= \mathbf{B}_i \mathbf{x}_i^{OH} \\ &= [\mathbf{b}_1^i, \dots, \mathbf{b}_{m_i}^i] \mathbf{x}_i^{OH} \\ &= \begin{bmatrix} b_{1,1}^i & \cdots & b_{1,C_i}^i \\ \vdots & \ddots & \vdots \\ b_{D,1}^i & \cdots & b_{D,C_i}^i \end{bmatrix} \begin{bmatrix} 0 \\ \vdots \\ 1 \\ 0 \\ \vdots \end{bmatrix} \end{aligned} \quad (2.3)$$

where $\mathbf{B}_i \in \mathbb{R}^{D \times C_i}$ is the embedding matrix for feature x_i , whose dimensions are determined by the chosen embedding dimension D and the cardinality of the feature, C_i . For numerical features in \mathbf{x} the cardinality is $C_i = 1$, so the embedding operation in equation 2.3 simply reduces to a scalar multiplication of feature value x_i and embedding

vector $\mathbf{b}_i \in \mathbb{R}^D$. The embedding matrix \mathbf{B}_i can either be derived by common dimensionality reduction methods such as Singular Value Decomposition, Principle Component Analysis, and Non-Negative Matrix Factorization, or by including \mathbf{B}_i in the set of trainable parameters in the gradient descent algorithm during model fitting (Hancock and Khoshgoftaar, 2020). The embedded feature representation $\hat{\mathbf{x}}$ that then gets fed into the model is then composed of a concatenation of all sparse feature embeddings \mathbf{e}_i dense numerical feature values:

$$\hat{\mathbf{x}} = [\mathbf{e}_1, \dots, \mathbf{e}_n] \in \mathbb{R}^{\tilde{n}} \quad (2.4)$$

where $\tilde{n} = D \cdot n$ is the resulting dimensionality of $\hat{\mathbf{x}}$. However, it has been shown that even when using embeddings, constructing a model that learns the key informative patterns in highly sparse data still proves to be an extremely difficult task (Gu, 2021; Zhang et al., 2021). This is indeed the key challenge behind building an accurate CTR prediction model, and is a key motivating factor as to why Deep Neural networks have outperformed the classical shallow counterparts. This transition will be examined in more detail in sections 2.2 to 2.6.

2.2. Shallow CTR Models

2.2.1. Logistic Regression

The earliest examples of CTR classification models incorporated classical “shallow” (single layer) statistical regression methods. The most basic example of this was the **Logistic Regression** model, as implemented by Richardson et al. (2007) on advertisement data from the Microsoft Search engine. The LR model is composed by modelling the *log-odds* (also referred to as the *logit*) of a positive binary label as a linear combination of all of the respective feature values:

$$f_{\Theta}^{LR}(\tilde{\mathbf{x}}) = \theta_0 + \sum_{j=1}^{\tilde{n}} \theta_j \tilde{x}_j \quad (2.5)$$

where $f_{\Theta}^{LR} : \mathbb{R}^{\tilde{n}} \rightarrow \mathbb{R}$ represents the Logistic regression model parametrized by $\Theta = (\theta_0, \dots, \theta_{\tilde{n}})$. The benefits of the LR model are that due to its simplicity and low number of parameters, it is relatively easy to train in computational terms and also relatively easy to deploy (Zhang et al., 2021). However, the formulation in equation 2.5 reveals that the LR model does not explicitly account for *feature interactions*. As outlined in section 2.1, the categorical features tend to have a high cardinality, resulting in highly sparse feature embeddings. Many of the important patterns for CTR prediction are therefore likely to be expressed in terms of *combinations of features* rather than the individual feature values themselves. For example, a user’s tendency to click on a given advertisement is likely to be influenced by the *combination* of the category of good or service the given advertisement is trying to sell (e.g. premium fashion retail, travel, electronics et. cetera) and the demographic/socio-economic category that the given user

falls into (e.g. university student, young professional, retiree). These features combinations (and the corresponding combination of respective field values in the preprocessed feature vector $\tilde{\mathbf{x}}$) are commonly referred to in the literature as *cross-features* (Zhang and Zhang, 2023) or more commonly *feature interactions* (Cheng et al., 2016; Song et al., 2019; Xiao et al., 2017).

Whilst it is possible to incorporate feature interactions in an LR model through feature engineering, this quickly becomes infeasible for large sparse datasets. A number of techniques have been developed to automate the necessary feature engineering steps for this, either by implicitly assigning a weight to all second order feature interactions (Chang et al., 2010) or by utilizing Gradient Boosted Decision Trees to pick out the key interactions (Cheng et al., 2014). Unfortunately, the prior still tends to exhibit poor performance with sparse data, whereas the fact that the Gradient Boosting algorithm for the latter is difficult to parallelize makes this solution difficult to scale in many applications in practice (Zhang et al., 2021).

2.2.2. Factorization Machines

Factorization Machines first proposed by Rendle (2010) can be thought of as an extension of the Logistic Regression framework in equation 2.5 with additional terms that explicitly account for the interactions between different features. Its relative simplicity and computational scalability has made it a widely popular framework for CTR modelling (Gu, 2021). A 2-way (maximum feature interaction degree of 2) Factorization Machine model is formulated as:

$$f_{\Theta}^{FM^2}(\tilde{\mathbf{x}}) = \theta_0 + \sum_{j=1}^{\tilde{n}} \theta_j \tilde{x}_j + \sum_{j=1}^{\tilde{n}} \sum_{k=j+1}^{\tilde{n}} \langle \mathbf{v}_j, \mathbf{v}_k \rangle \tilde{x}_j \tilde{x}_k \quad (2.6)$$

where $\langle \cdot, \cdot \rangle$ represents the inner product between two vectors, the final interaction term above is parametrized by $\mathbf{V} \in \mathbb{R}^{\tilde{n} \times F}$. Each row \mathbf{v}_j of \mathbf{V} represents the j -th feature in $\tilde{\mathbf{x}}$ in terms of F latent factors. The factorization matrix \mathbf{V} is typically fitted by optimizing the binary cross-entropy loss function by means of Stochastic Gradient Descent. It is intuitive to see that \mathbf{V} will be fitted such that if the interaction between feature j and k have a positive impact on $p(y)$, then j -th and k -th rows of \mathbf{V} will have positive inner products (and vice versa) (Zhang et al., 2021).

Rendle (2010) shows that although direct evaluation of equation 2.6 would appear to have a complexity of $O(F\tilde{n}^2)$, the 2-way FM model in fact scales linearly in \tilde{n} and F :

Lemma 2.2.1. The model equation of a 2-way factorization machine (eq. 2.6) can be computed in linear time $O(F\tilde{n})$.

Proof.

Due to the factorization of the pairwise interactions, there is no model parameter that directly depends on two features (j, k) . This means that pairwise interactions can be reformulated as such

$$\begin{aligned}
& \sum_{j=1}^{\tilde{n}} \sum_{k=j+1}^{\tilde{n}} \langle \mathbf{v}_j, \mathbf{v}_k \rangle \tilde{x}_j \tilde{x}_k \\
&= \sum_{j=1}^{\tilde{n}} \sum_{k=j+1}^{\tilde{n}} \sum_{f=1}^F v_{j,f} v_{k,f} \tilde{x}_j \tilde{x}_k \\
&= \frac{1}{2} \left(\sum_{j=1}^{\tilde{n}} \sum_{k=1}^{\tilde{n}} \sum_{f=1}^F v_{j,f} v_{k,f} \tilde{x}_j \tilde{x}_k - \sum_{j=1}^{\tilde{n}} \sum_{f=1}^F v_{j,f} v_{j,f} \tilde{x}_j \tilde{x}_j \right) \\
&= \frac{1}{2} \sum_{f=1}^F \left(\sum_{j=1}^{\tilde{n}} v_{j,f} \tilde{x}_j \sum_{k=1}^{\tilde{n}} v_{k,f} \tilde{x}_k - \sum_{j=1}^{\tilde{n}} v_{j,f}^2 \tilde{x}_j^2 \right) \\
&= \frac{1}{2} \sum_{f=1}^F \left(\left(\sum_{j=1}^{\tilde{n}} v_{j,f} \tilde{x}_j \right)^2 - \sum_{j=1}^{\tilde{n}} v_{j,f}^2 \tilde{x}_j^2 \right)
\end{aligned}$$

The complexity of the final line above is $O(F\tilde{n})$, and hence the FM formulation as per equation 2.6 scales linearly in F and \tilde{n} . \square

This quality greatly simplifies the computational complexity of scaling the FM model to larger datasets with a more sparse categorical features. Moreover, the Factorization Machine framework can be generalized to degree R (i.e. up to any limit of feature interaction order) as follows:

$$f_{\Theta}^{FM^R} = \theta_0 + \sum_{j=1}^{\tilde{n}} \theta_j \tilde{x}_j + \sum_{r=1}^R \sum_{j_1=1}^{\tilde{n}} \cdots \sum_{j_r=j_{r-1}+1}^{\tilde{n}} \left(\prod_{k=1}^r \tilde{x}_{j_k} \right) \left(\sum_{f=1}^{F_r} \prod_{k=1}^r v_{j_k,f}^{(r)} \right) \quad (2.7)$$

The FM framework therefore provides an intuitive and computationally scalable method to account for key feature interactions without the need of extensive feature engineering. Extensions and improvements to FM have been proposed, most notably in the form of the Field-Aware Factorization Machine (FFM) framework by Juan et al. (2016), which only accounts for interactions between features of different fields (in otherwords, it ignores the interaction between \tilde{x}_j and \tilde{x}_k if both are components of embedding vector embed_i for some categorical feature x_i) as well as Gradient Boosted Factorization Machines (Cheng et al., 2014), which again aims to augment the FM framework by means of the Gradient Boosting algorithm.

2.3. Introducing MLPs in CTR prediction

Despite the advantages of the FM framework, a setback of the formulation in equation 2.7 is that the framework grows highly complex and overparametrized for higher

values of R . As a consequence, only the 2-way FM framework as per equation 2.6 tends to be implemented in practice, meaning that the FM model alone is practically insufficient for capturing feature interactions of order $\gg 2$ (Guo et al., 2017). Deep Neural Networks present a powerful alternative for addressing this shortcoming. Neural networks benefit from being universal function approximators (Cybenko, 1989) and from the fact that neural network batch training is paralellizable by means of GPU accelerated computation. This has lead to the successfull application of Deep Learning algorithms across multiple fields such as Natural Language Processing and Image classification (He et al., 2016; Krizhevsky et al., 2017; LeCun et al., 1998). These factors and successes showed that DNN's have the potential to extract informative feature representations from highly sparse and abstract data, and as a consequence, the application of DNN's in CTR prediction started recieving attention in the mid-2010's.

The **Multilayer Perceptron** (MLP) is the most elementary type of Deep Neural Network (Webster, 2024). In general, a MLP with L hidden layers is formulated as such:

$$\mathbf{h}^{(0)} := \tilde{\mathbf{x}} \quad (2.8)$$

$$\mathbf{h}^{(l)} = \phi_l \left(\mathbf{W}^{(l-1)} \mathbf{h}^{(l-1)} + \mathbf{b}^{(l-1)} \right), l = 1, \dots, L \quad (2.9)$$

$$\hat{y} = \phi_{out} \left(\mathbf{w}^{(L)} \mathbf{h}^{(L)} + b^{(L)} \right) \quad (2.10)$$

where $\mathbf{W}^{(k)} \in \mathbb{R}^{n_{l+1} \times n_l}$, $\mathbf{b}^{(k)} \in \mathbb{R}^{n_{l+1}}$, $\mathbf{h}^{(l)} \in \mathbb{R}^{n_l}$, $n_0 = \tilde{n}$, n_l is the number of hidden units in layer l and ϕ_l is the activation function for layer l , When rearranged in the form of equation 2.1, the above becomes:

$$f_{\Theta}^{MLP}(\tilde{\mathbf{x}}) = \psi_{out}(\psi_L(\dots \psi_1(\tilde{\mathbf{x}}) \dots)) \quad (2.11)$$

where each function ψ_l represents the affine transformation and element-wise activation operation for layer l . MLPs can be thought of as an acyclic graph, as displayed in Figure 2.2. The data $\tilde{\mathbf{x}}$ first gets fed through the *input layer*, then gets processed by multiple *hidden layers* that include a series of affine transfromations followed by activation functions, before the final result is produced by the *output layer*.

Figure 2.2 demonstrates the potential that DNN's have for modelling higher order feature interactions. By training the network by means of Stochastic Gradient Descent, it should be possible to calculate the appropriate weight (\mathbf{W}_l) and bias (\mathbf{b}_l) parameters in order capture the relevant high-order feature patterns in the data. As such, many CTR modelling frameworks have been developed that use Deep Learning techniques to build upon and imporved the previously discussed classical methods by incorporating Deep Neural Networks such as the ML in the model architecture (Zhang et al., 2021).

2.4. Single vs Dual Tower Architectures

Before moving on to DNN enhanced CTR models in section 2.5 it is worth briefly discussing the difference between **Single-Tower** models and **Dual-Tower** architecture



Figure 2.2.: Multilayer Perceptron with two hidden layer. Taken from (Webster, 2024)

models. Single Tower models place all layers successively in the architecture, and can generally be formulated as in equation 2.11. Since all feature inputs are passed through the same set of successive affine transformations and activations, Single Tower models are usually able to capture higher order feature interactions, but the signal from the low-order interactions tend to be lost (Zhang et al., 2021). The FNN (Zhang et al., 2016), FGCNN (Liu et al., 2019) and PNN (Qu et al., 2016) models covered in the subsections 2.5 and 2.6 are examples of Single Tower models.

In order to avoid diluting the signal from the lower order feature interactions, many architectures adopt a Dual Tower architecture, as shown on the right-hand side of Figure 2.3. A separate **Feature Interaction Layer** is placed parallelly to the DNN, and the final output is composed of a weighted sum of the feature interaction and DNN outputs. With this architecture, the feature interaction layer is usually dedicated to capturing the important lower order feature interaction signals, whereas the DNN acts as a *residual network* for capturing any meaningful signals that may be missing. As a result, Dual Tower networks tend to benefit from better training stability and better performance (Zhang et al., 2021).

2.5. DNN Enhanced CTR models

2.5.1. Factorization-machine Supported Neural Networks

One of the earliest example of the use of Deep Neural Networks being used to enhance existing CTR modeling methods is the **Factorization-machine Supported Neural Network** (FNN) (Zhang et al., 2016). The FNN model is a Single Tower model that works by pretraining a 2-way Factorization Machine model as in equation 2.6 on the concatenated one-hot encoded categorical feature vectors, and then using the feature interaction vectors and weights as the embedding matrix.

Below we start with the feature vector with one-hot encoded categorical feature rep-

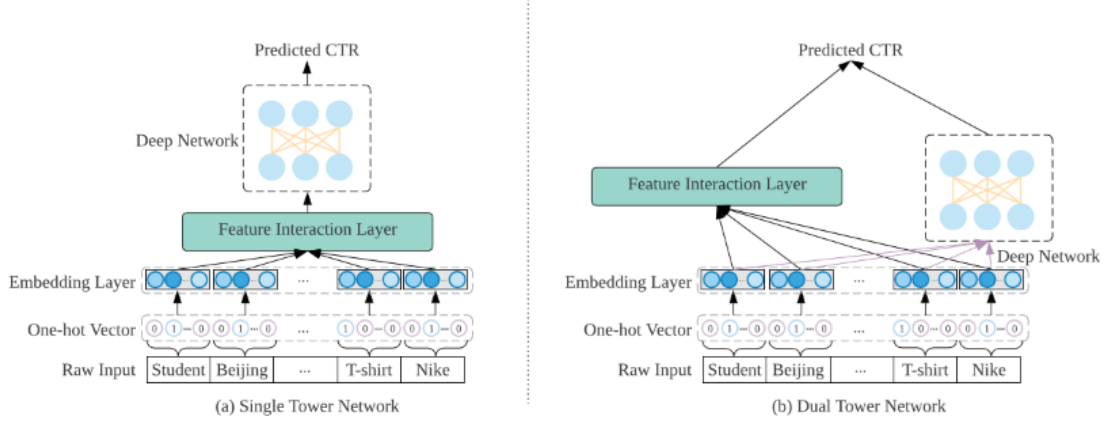


Figure 2.3.: Single vs Dual Architecture Networks. Source: (Zhang et al., 2021)

representations, and then *prefit* a 2-way Factorization Machine model as in section 2.2:

$$\tilde{\mathbf{x}} = [\mathbf{x}_1^{OH}, \dots, \mathbf{x}_s^{OH}, x_{s+1}, \dots, x_{s+d}]$$

$$f_{\Theta}^{FM^2}(\tilde{\mathbf{x}}) = \theta_0 + \sum_{j=1}^{\tilde{n}} \theta_j \tilde{x}_j + \sum_{j=1}^{\tilde{n}} \sum_{k=j+1}^{\tilde{n}} \langle \mathbf{v}_j, \mathbf{v}_k \rangle \tilde{x}_j \tilde{x}_k$$

We then use the weights and biases from $\Theta = (\theta_0, \theta_1, \dots, \theta_{\tilde{n}}, \mathbf{v}_1, \dots, \mathbf{v}_{\tilde{n}})$ to derive the feature embedding as follows:

$$\tilde{\mathbf{x}} = [\theta_0, \mathbf{e}_1, \mathbf{e}_2, \dots, \mathbf{e}_{s+d}]$$

where each embedding vector \mathbf{e}_i is defined as the concatenation of the weight (θ_j) and FM interaction vector (\mathbf{v}_j), where j is chosen to be the index for $\tilde{\mathbf{x}}$ that corresponds to the non-zero value in one-hot field i in $\tilde{\mathbf{x}}$:

$$\mathbf{e}_i = [\theta_j, \mathbf{v}_j], \text{ such that } start_i \leq j < end_i \text{ and } \tilde{x}_j = 1$$

The above can alternatively also be recovered from equation 2.3 by defining a *field-wise* embedding matrix \mathbf{B}_i to a $(D+1) \times C_i$ matrix with the following values

$$\mathbf{B}_i = \begin{bmatrix} b_{1,1}^i & \dots & b_{1,C_i}^i \\ \vdots & \ddots & \vdots \\ b_{D+1,1}^i & \dots & b_{D+1,C_i}^i \end{bmatrix} = \begin{bmatrix} \theta_1^i & \dots & \theta_{C_i}^i \\ v_{1,1}^i & \dots & v_{1,C_i}^i \\ \vdots & \ddots & \vdots \\ v_{D,1}^i & \dots & v_{D,C_i}^i \end{bmatrix}$$

where θ_c^i represents the feature weight for the c -th feature in field i in $\tilde{\mathbf{x}}$, and $\mathbf{v}_c^i = (v_{1,c}^i, \dots, v_{D,c}^i)$ is the FM interaction vector for the c -th feature in field i in $\tilde{\mathbf{x}}$. Then, if we define $\tilde{\mathbf{x}}[start_i : end_i] = x_i^{OH}$, then \mathbf{e}_i can be defined as:

$$\mathbf{e}_i = (\mathbf{B}_i \tilde{\mathbf{x}}[start_i : end_i]^\top)^\top = [\theta_j, \mathbf{v}_j]$$

Figure 2.4 portrays the structure of this model as it was presented in the original paper by Zhang et al. (2016).

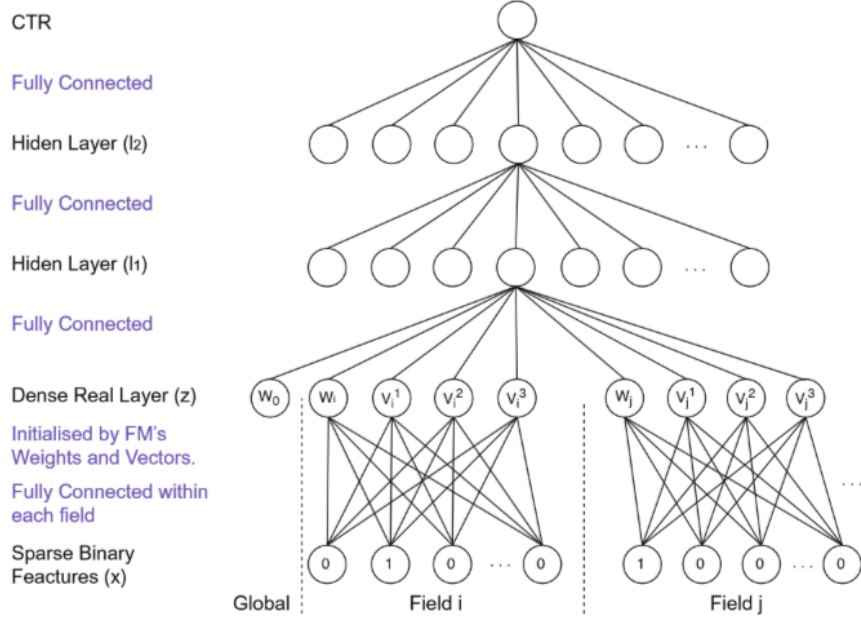


Figure 2.4.: FNN model architecture. Source: (Zhang et al., 2016)

By incorporating the FM model feature interaction vectors in the embedding layer before the DNN, the FNN model is able to leverage the FM model's strength in interaction identification. The FNN model then leverages a MLP network to capture the higher order interaction signals much more efficiently than would have been feasibly possible when relying only on FM. Because of this, comprehensive experiments carried out by Zhang et al. (2016) confirmed that FNN has superior CTR estimation performance than both LR and FM.

However Guo et al. (2017) and Zhang et al. (2021) find that due to its Single Tower architecture, lower-order feature interaction signals tend to be lost in the network. Guo et al. (2017) further found that the FM pretraining step described above represents a significant overhead in terms of training efficiency. In the next subsections, we will see how the Wide & Deep and DeepFM models aim to solve for these issues.

2.5.2. Wide and Deep

The **Wide and Deep Learning** (WDL) model was developed by Cheng et al. (2016).

$$f_{\Theta}^{W\&D} = \theta_0 + \sum_{k=1}^{\hat{n}} \theta_k \hat{\mathbf{x}}_k + f_{\Phi}^{MLP}(\tilde{\mathbf{x}}) \quad (2.12)$$

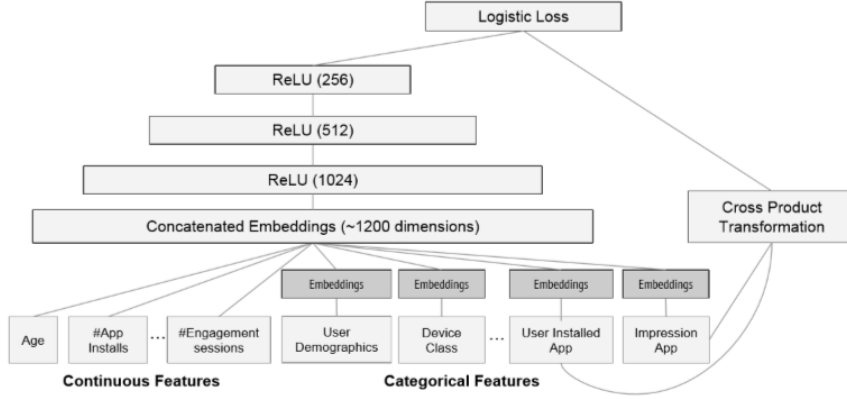


Figure 2.5.: Wide and Deep Learning Model, as illustrated in (Shen, 2017)

Figure 2.5 reveals that the W&D model is composed with a Dual-Tower Architecture, with a Deep Component and a Wide Component (shown on the left and right hand sides of Figure 2.5 respectively). The Deep Component is composed of a MLP with multiple hidden layers, each with the Rectified Linear Unit (ReLU) activation function. The Wide Component is formulated by the first two terms in equation 2.12, and is composed of a simple linear transformation of the input features. The key aspect of the Wide Component is the fact that the linear transformation is not simply applied to the encoded features $\tilde{\mathbf{x}}$, but instead to these concatenated with a set of cross-product transformed features. In other words:

$$\hat{\mathbf{x}} = [\tilde{\mathbf{x}}, v_1(\tilde{\mathbf{x}}), \dots, v_P(\tilde{\mathbf{x}})] \quad (2.13)$$

Where $v_k(\tilde{\mathbf{x}}) = \prod_{j=1}^{\hat{n}} \tilde{x}_j^{c_{kj}}$ and $c_{kj} \in \{0, 1\}$.

Consequentially of equation 2.13, the Wide Component *memorizes* the key feature interactions that are defined by the specific *cross-product transformations* ($v_k(\tilde{\mathbf{x}})$) (Cheng et al., 2016). Meanwhile, the Deep Component captures any residual signals that may not have been explicitly included in the manually defined cross-product transformations (Zhang et al., 2021). In this sense, the W&D model overcomes the shortcomings of the FNN model, by having dedicated pathways in the architecture for higher and lower order feature interactions. However, the downside of W&D is the fact that the feature interactions in the Wide component need to be manually incorporated by defining the cross-product transformation functions $\{v_k(x)\}_{k=1}^P$. This means that there is a significant feature engineering component that would be necessary to use this model effectively.

2.5.3. DeepFM

The **DeepFM** model was developed by Guo et al. (2017) in order to address the shortcomings of the FNN and W&D models mentioned in this section, as well as those of the PNN model which will be covered in section 2.6. Similarly to the WDL model, the DeepFM network two components arranged as a Dual Tower architecture, as visualized in Figure 2.6.



Figure 2.6.: DeepFM network architecture. Source: (Shen, 2017)

The *FM component* effectively replaces the Wide component in the WDL model. It consists of a 2-way Factorization Machine layer that models pairwise feature interactions between the different fields of $\tilde{\mathbf{x}}$ as inner products of the respective feature latent vectors \mathbf{v}_j (Guo et al., 2017). Due to the linear scalability of the FM discussed in section 2.2, the FM component can effectively capture important order-2 feature interactions automatically, without the need to manually define cross-product functions as in the case of the W&D model.

Meanwhile, the *Deep component* fulfills a similar purpose as in the case of the WDL model. The deep component is a MLP network that takes the feature embedding vector $\tilde{\mathbf{x}}$ as inputs, and learns the higher-order feature interactions that cannot be captured by the 2-way FM component. Like with the WDL model, the Deep component acts as a residual network for capturing signals that were omitted by the FM component. The DeepFM model can therefore be formulated as in equation 2.14.

$$f_{\Theta}^{\text{DeepFM}} = f_{\Phi}^{\text{FM}^2}(\tilde{\mathbf{x}}) + f_{\Omega}^{\text{MLP}}(\tilde{\mathbf{x}}) \quad (2.14)$$

A notable difference in the Deep components between the WDL and DeepFM models

are in the construction of the embedding layers that preprocess the input to the MLP. In DeepFM, the latent feature vectors (\mathbf{V}) are trainable network weights that are derived during SGD optimization in the FM component. For every successive step in the model training, the learned latent feature vectors are used in the embedding layer that preprocesses that raw input features before the MLP of the Deep component (see Figure 2.7). This is similar to how the feature embeddings were derived in the FNN model (Zhang et al., 2016), except for fact the FM layer is included in the overall learning architecture of the model. This eliminates the need to pretrain the FM model, thereby allowing for the FM latent feature vectors to be learned concurrently during the overall DeepFM model training procedure (Guo et al., 2017).

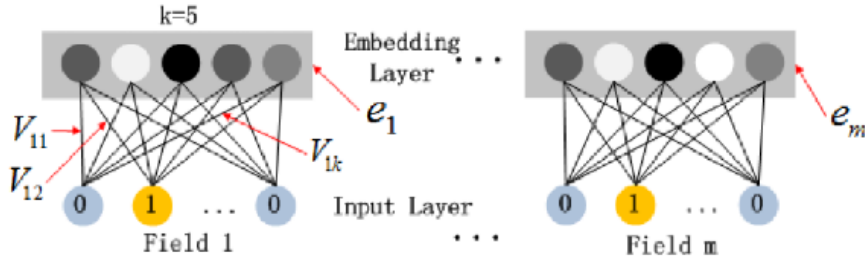


Figure 2.7.: The embedding layer of the Deep Component in the DeepFM model. Source: (Guo et al., 2017)

The key benefits of the DeepFM model are threefold. Firstly, we have already mentioned above that the fact that the FM model is incorporated directly into the model architecture eliminates the need to pretrain the FM latent feature vectors, thereby eliminating the computational overhead that is necessary for this in the case of FNN (Zhang et al., 2016). Secondly, the Dual Tower architecture allows the model to simultaneously learn both low as well as high order feature interactions. Thirdly, the previously discussed computational efficiency of the FM model means that DeepFM is relatively scalable in terms of the number of features and the size of the latent embedding space, especially in comparison to the Product based Neural Network (PNN) models (Qu et al., 2016), which will be covered in section 2.6.

2.6. Feature Interaction Operator Models

MLPs have been proven to be universal function approximators, meaning that any function can be sufficiently approximated with a larger enough MLP (Cybenko, 1989; Hornik et al., 1989, 1990). However, Shalev-Shwartz et al. (2017) found that for complex problems where the true target function is actually a larger set of uncorrelated solution functions, Deep Neural Networks suffer from an *insensitive gradient issue* during gradient descent optimization. Shalev-Shwartz et al. (2017) show that when the target function is a set of uncorrelated functions, the variance of the gradient with respect to the target decreases linearly with respect to the number of functions that make up the target. The decrease in this variance has the effect of decreasing the correlation between

the gradient and the target, causing the optimization of the DNN to fail. Qu et al. (2018) argues that since the target function for the CTR classification task typically consists of a set of uncorrelated if-then classifiers on the basis sparse categorical features, the insensitive gradient issue is likely to be prevalent in cases where MLPs are relied upon directly to detect the key feature interactions in sparse CTR classification data.

The above justifies the design of specific layers and architectures that explicitly detect important feature interactions in the data. In this section, we discuss **Feature Interaction Operators**, which are deep learning layers that were developed specifically to assist the DNN in its capacity to learn higher feature interactions (Zhang et al., 2021). The three different type of Feature Interaction Operators that are discussed in this section are Product Operators, Convolutional Operators and Attention Operators.

2.6.1. Product Operators models

Product-based Neural Network

Product Operator networks are neural networks that include layers with inner or outer product operations in order to explicitly model feature interactions (Zhang et al., 2021). The **Product-based Neural Network** (PNN) introduced the concept of product operator models as it includes a product layer between the embedding layer and the MLP in order to model second order feature interactions in the data. All of this is arranged as a Single Tower architecture, as shown in Figure 2.8.

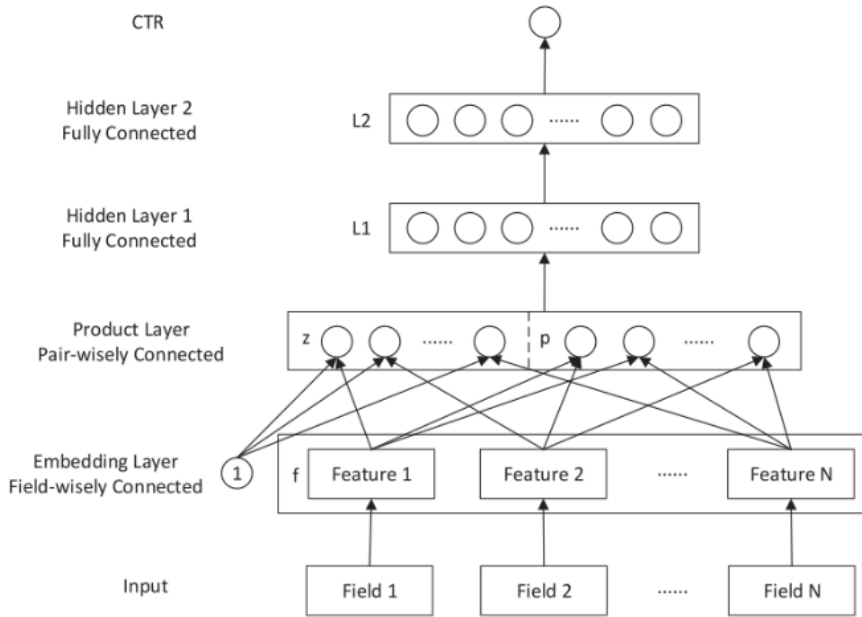


Figure 2.8.: Product-based Neural Network. Source: (Qu et al., 2016).

The key defining component of the PNN is the *Product Layer*. Each embedding field \mathbf{e}_i in the preceding embedded layer is pair-wisely connected to each of the other fields and a “1” constant signal. The output of the product signal can then be broken out into two parts:

- Virtue to the constant “1” signal, the first part is simply a vector \mathbf{z} that consists of a concatenation of all of the field embeddings. In other words $\mathbf{z} = \dot{\mathbf{x}}$.
- A second-order interaction vector, $\mathbf{p} = \{p_{i,j}\}$ where $i, j = 1, \dots, n$, where each element $p_{i,j} = g(\mathbf{e}_i, \mathbf{e}_j)$ defines a pairwise field interaction.

In their initial paper, Qu et al. (2016) proposed two variants of the PNN model, the Inner Product Based Neural Network and the Outer Product Based Neural Network, differentiated by whether g is the Inner or Outer product operation respectively. The \mathbf{z} and \mathbf{p} vectors are then both projected to \mathbb{R}^{D^1} space (the input dimension of the MLP network) by means of trainable weight matrices, W_z and W_p . The input to the MLP network is then the sum of the two resulting vectors and a bias vector \mathbf{b}_1 . The formulation for the PNN network is summarized in terms of $\dot{\mathbf{x}}$ in equation 2.15.

$$f_{\Theta}^{PNN}(\dot{\mathbf{x}}) = f_{\Phi}^{MLP}(W_z \dot{\mathbf{x}} + W_p \mathbf{p} + \mathbf{b}_1) \quad (2.15)$$

The inclusion of the product layer in the PNN model automatically incorporates second order field-wise interactions as inputs to the MLP by means of inner or outer products, thereby partially alleviating the previously mentioned insensitive gradient issue. Qu et al. (2016) found that as a result of this, the PNN models outperformed LR, FM, FNN and the CCPM models in terms of Log Loss and AUC. However, a major disadvantage of the product layer operations is the computational time complexity, which increases quadratically with the number of fields and the embedding dimension. In order to alleviate this, Qu et al. (2016) implement simplified versions of the inner and outer product computations (in which some neurons are eliminated in the inner product, and the result for the outer product is compressed for all fields at once), but even then the PNN models still tend to be less computationally efficient than its peers. Furthermore, since the PNN model leverages a Single Tower architecture it suffers from the same issue as the FNN model wherein the lower order interactions are ignored.

Neural Factorization Machine

The **Neural Factorization Machine** (NFM) model introduced by He and Chua (2017) works on a similar principle to PNN, in that it also has a product layer in its architecture. The NFM model calculates the pre-sigmoid prediction as in equation 2.16:

$$f_{\Theta}^{NFM}(\tilde{\mathbf{x}}) = w_0 + \sum_{j=1}^{\tilde{n}} \tilde{x}_j + f_{\Phi}^{NFM-Deep}(\tilde{\mathbf{x}}) \quad (2.16)$$

Recall that here, $\tilde{\mathbf{x}}$ is a sparse vector composed of concatenated one-hot categorical feature fields, as well as the numerical features in \mathbf{x} . The first two terms in equation 2.16

are simply composed of a bias parameter w_0 , and a linear combination of the feature values in $\tilde{\mathbf{x}} = (\tilde{x}_1, \dots, \tilde{x}_n)$. The last term in equation 2.16 represents the core component of the NFM model, and includes an architecture similar to that of the PNN model with an embedding layer, a unique type of product layer called a *Bi-Interaction Pooling Layer* followed by a multi-layer MLP network. The architecture for $f_{\Phi}^{NFM-Deep}$ is visualized in Figure 2.9.

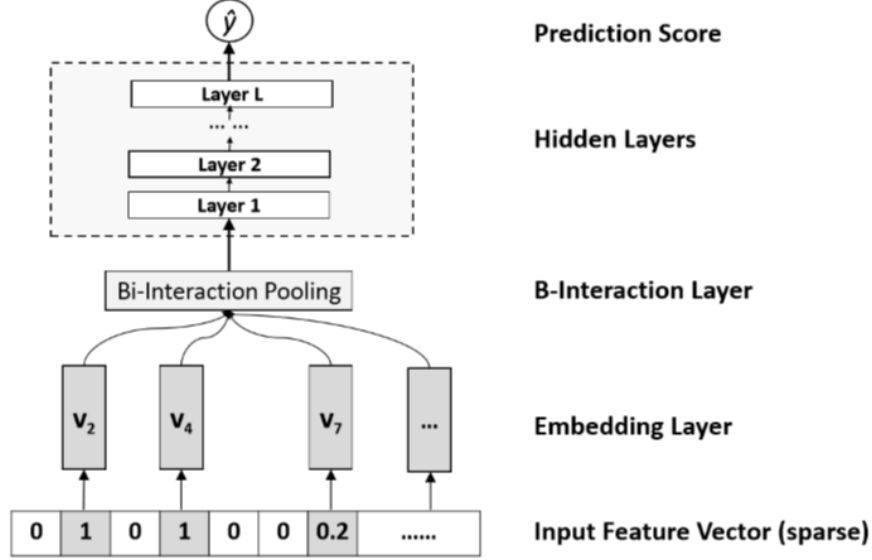


Figure 2.9.: Neural Factorization Machines model excluding the first-order linear regression part. Source: He and Chua (2017)

The *Embedding Layer* in Figure 2.9 is a fully connected layer that carries out the embedding operation described in equation 2.3. The *Bi-Interaction Pooling* layer then takes the embedded feature vector $\hat{\mathbf{x}}$ produced by the embedding layer as input and combines all of the respective feature embeddings $\{\mathbf{e}_i\}_{i=1}^n$ into a single feature vector by the following operation:

$$f^{BI}(\{\mathbf{e}_i\}_{i=1}^n) \sum = \sum_{j=i+1}^n \mathbf{e}_i \odot \mathbf{e}_j \quad (2.17)$$

where \odot represents the element-wise product of two vectors. The benefit of the Bi-Interaction Pooling layer is its efficiency. It does not introduce any additional model parameters and can be calculated in linear time. Equation 2.17 can be reformulated as:

$$f^{BI}(\{\mathbf{e}_i\}_{i=1}^n) \sum = \frac{1}{2} \left[\left(\sum_{i=1}^n \mathbf{e}_i \right)^2 - \sum_{i=1}^n (\mathbf{e}_i)^2 \right]$$

When considering the feature cardinalities C_i and the embedding dimension D , the above calculation can be performed in $O(n)$ time He and Chua (2017). The NFM model

therefore benefits from better training efficiency and stability in comparison to most other Deep Learning methods, while simultaneously being able to capture both feature interactions through the $f_{\Phi}^{NFM-Deep}$ as well as key feature signals through the linear components of equation 2.16 (Zhang et al., 2021).

Deep & Cross Network

Neither the PNN nor the NFM models guarantee that each order of feature interaction will be modelled. The **Deep & Cross Network** (DCN) developed by Wang et al. (2017) applies feature crossing at each layer and efficiently learns predictive cross features to a hyperparametrized bounded degree without requiring additional feature engineering. The DCN model is has a Dual-Tower architecture comprised of a Cross Network and a Deep Network, as shown in Figure 2.10.

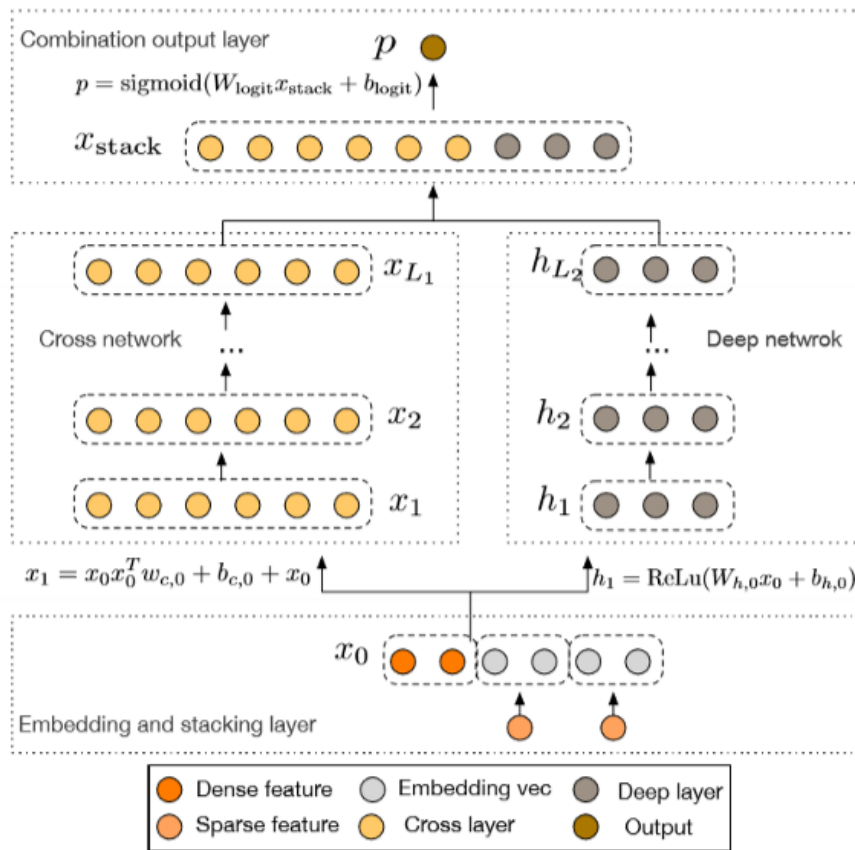


Figure 2.10.: Deep & Cross Network model. Source: (Wang et al., 2017)

The Cross Network and Deep Networks are both preceded by an Embedding and Stacking layer, which produces a vector containing concatenated categorical feature embeddings \mathbf{e}_i and normalized numerical feature embeddings x_i . The Deep Network

consists of a standard Multilayer Perceptron component with ReLu activation. The Cross Network is composed of L cross layers, where the output of each cross layer \mathbf{x}_{l+1} is calculated as:

$$\mathbf{x}_{l+1} = \mathbf{x}_0 \mathbf{x}_l^\top \mathbf{w}_l + \mathbf{b}_l + \mathbf{x}_l \quad (2.18)$$

where \mathbf{x}_0 is the output of the Embedding and Stacking layer and $\mathbf{w}_l, \mathbf{b}_l$ are trainable weight and bias parameter vectors for each cross layer. Wang et al. (2017) show linking crossing operations formulated by equation 2.18, the output of a L -layer Cross Network comprises explicitly of cross-feature terms of degrees 1 to $L + 1$.

2.6.2. Convolutional Operator Models

Convolutional Click Prediction Model

Convolutional Operator Models use the convolution operation to extract key local-global features from the categorical field embeddings. The earliest and most well known example of a Convolutional Operator model is the **Convolutional Click Prediction Model** (CCPM) developed by Liu et al. (2015). The overall architecture of this model was shown in the original paper as in Figure 2.11.

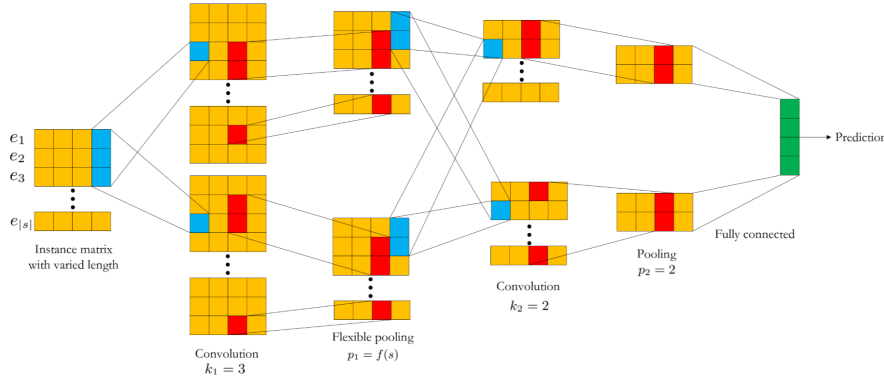


Figure 2.11.: Convolution Click Prediction Model architecture. Source: (Liu et al., 2015).

The input to the CCPM model consists of a $s \times D$ dimensional matrix of stacked categorical feature embeddings, as shown on the left-hand side of Figure 2.11. Per the standard architecture discussed in (Liu et al., 2015), this matrix is then passed through a series of Convolutional and Pooling layers. The number of maximum features that the intermediate pooling layers take is flexible to account for the flexible input matrix length. The final prediction is calculated by passing the final pooling result through a MLP, shown on the right-hand side of Figure 2.11 in green. This makes the CCPM model a Single Tower architecture model that can be roughly summarized as per equation 2.19.

$$f_{\Theta}^{CCPM}(\tilde{\mathbf{x}}) = f_{\Phi}^{MLP}(f_{\Omega}^{Conv}(\tilde{\mathbf{x}})) \quad (2.19)$$

where f_{Ω}^{Conv} represents the series of convolutions and pooling layers described above.

Liu et al. (2015) show that the CCPM model outperforms the LR, FM and RNN models in terms of Log Loss/Binary Cross-Entropy. However, a common criticism of the CCPM model is that due to the equivariance property of the Convolution operations, the degree to which it is able to capture important feature interactions in the data is highly dependant on how the features are ordered in the input matrix (Gu, 2021; Qu et al., 2018; Zhang et al., 2021). Convolutions by nature extract feature maps in the local neighbourhood of each variable, but fail to do so globally.

Feature Generation by Convolutional Neural Network

The **Feature Generation by Convolutional Neural Network** model proposed by Liu et al. (2019) introduces a *feature recombination layer* to mitigate this issue. The architecture for the FGCNN model is shown in Figure 2.12

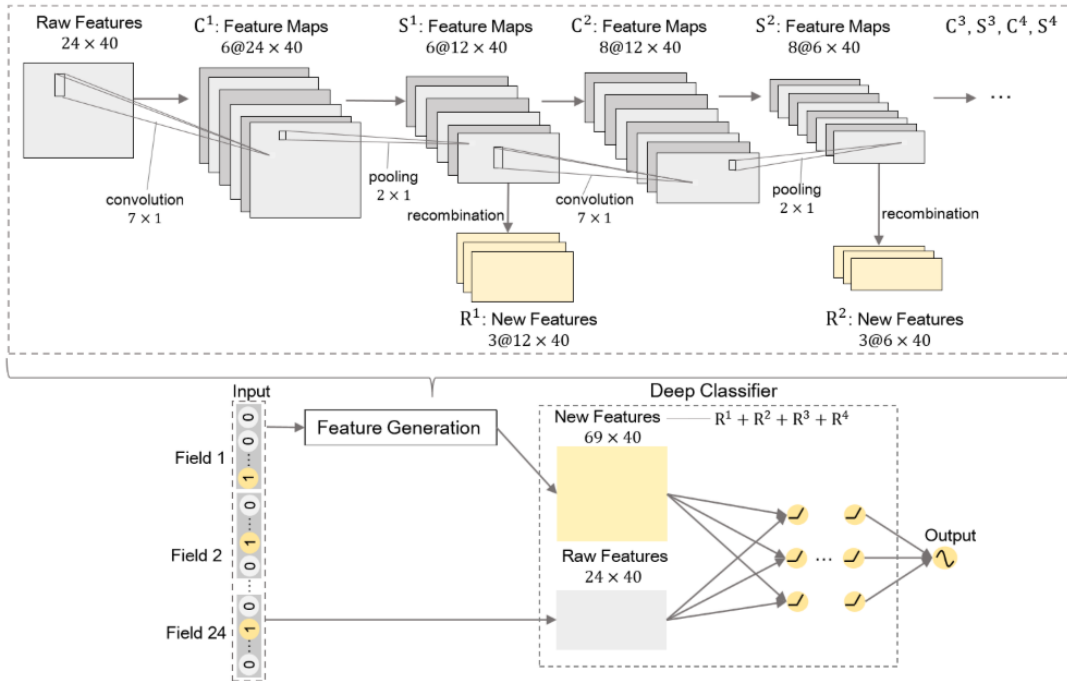


Figure 2.12.: FGCNN model architecture with Feature Generation Component. Source: (Liu et al., 2019)

The main body of the FGCNN model consists Deep Classifier that is essentially an Inner Product Neural Network, which was discussed above (Qu et al., 2018). The inputs to the Deep Classifier consist of the input feature embeddings ($\tilde{\mathbf{x}}$), concatenated with a set of new features that are created in the Feature Generation component of the model. This Feature Generation component represents the primary innovation of the FGCNN model, and is visualized at the top of Figure 2.12. As with CCPM, the Feature

Generation component is composed of a series of two dimensional convolutional and max pooling layers, and takes the input feature embedding matrix as an input. However, in order to solve for the input order dependency issue prevalent with CCPM, the resulting feature maps are first passed through a fully connected *recombination layer* that models non-adjacent interactions.

2.6.3. Attention Operator Models

Attention Operator Models aim to utilize the attention mechanism for identifying the key feature interactions in the data. The **Autotomatic Feature Interaction Learning** (AutoInt) model proposed by Song et al. (2019) makes use of a multi-head self attention network to model the important feature interactions in the data. The initial paper separates the model into three parts: an embedding layer, an interaction layer and an output layer. The embedding layer aims to project each sparse multi-value categorical and dense numerical feature into a lower dimensional space, as per the below:

$$\mathbf{e}_i = \frac{1}{q} \mathbf{V}_i \mathbf{x}_i$$

where \mathbf{V}_i is the embedding matrix for the i -th field, x_i is a multi-hot vector, and q is the number of non-zero values in x_i . The interaction layer employs the multi-head mechanism to determine which higher order feature interaction are meaningful in the data. This not only improves the efficiency of model training, but it also improves the model's explainability. Lastly, the output layer is a fully connected layer that takes in the concatenated output of the interaction layer, and applies the sigmoid activation function to produce the final prediction. The architecture of the AutoInt model is shown in Figure 2.13.

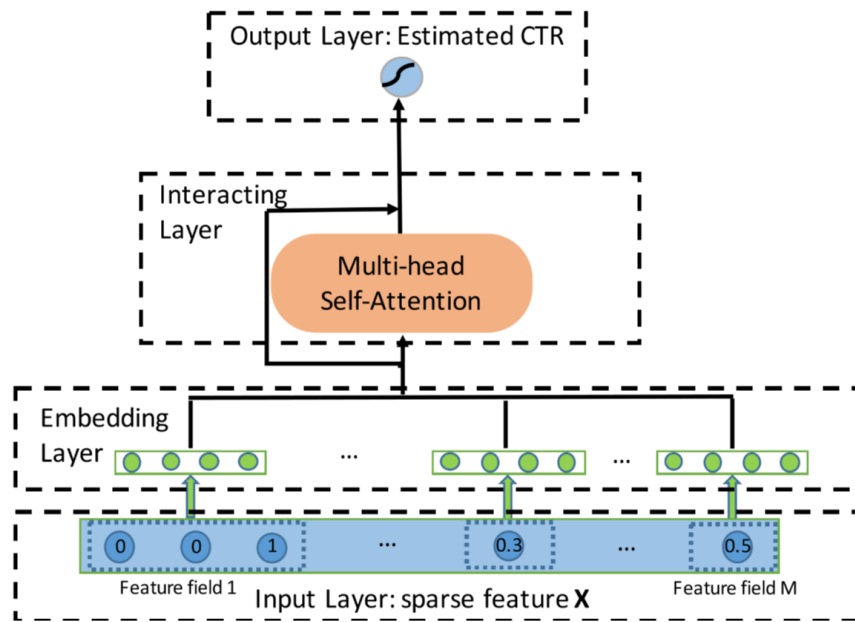


Figure 2.13.: The Automatic Feature Interaction Learning model architecture. Source: (Song et al., 2019)

3. Background: Deep Reinforcement Learning

The second part of the background material in this report is dedicated to Deep Reinforcement Learning. We first proceed by explaining the foundational concepts, in which we will establish definitions for Markov Decision Processes, Reinforcement Learning and Dynamic Programming. We then move on to explain Q-Learning, a specific class of Reinforcement Learning algorithms, as well as how Deep Learning models are being applied in the case of Deep Q-Learning. Finally, we introduce the Deep Reinforcement Learning News recommendation (DRN) algorithm (Zheng et al., 2018), a Q-learning algorithm which we have repurposed for ad recommendation.

3.1. RL Basics: MDPs and Bellman Optimality Equations

In the case of many online systems and applications where there is a series of interactions between users and the system, it is often desirable to find the optimal set of content to display to the users in order to maximize their engagement as time goes on. This problem can be framed as a **Markov Decision Process**. Definition 3.1.1 was taken from (Pike-Burke, 2024b) have been chosen for evaluation:

Definition 3.1.1. An episodic **Markov decision process** (MDP) is defined by tuple $\mathcal{M}(\mathcal{S}, \mathcal{A}, H, \nu, \{P_h\}_{h=1}^H, \{r_h\}_{h=1}^H)$ where:

- \mathcal{S} is the state space of finite cardinality.
- \mathcal{A} is the finite set of actions.
- $H \in \mathbb{N}$ is the horizon of the problem.
- ν is the initial state distribution.
- $\{P_h\}_{h=1}^H$ is the collection of transition functions where $P_h : \mathcal{S} \times \mathcal{A} \rightarrow \Delta(\mathcal{S})$ where $\Delta(\mathcal{S})$ is the set of probability distributions over \mathcal{S} . When action $a \in \mathcal{A}$ is taken from state $s \in \mathcal{S}$ at stage h , $P_h(s'|s, a)$ gives the probability of transitioning to state $s' \in \mathcal{S}$ for all $s' \in \mathcal{S}$.
- $\{r_h\}_{h=1}^H$ is the collection of reward functions, $r_h : \mathcal{S} \times \mathcal{A} \rightarrow [0, 1]$ where $r_h(s, a)$ gives the reward from taking action $a \in \mathcal{A}$ from state $s \in \mathcal{S}$ at stage $h \in \{1, \dots, H\}$.

To relate the above to the Ad marketplace context, we can adopt the language introduced in section 2.1. Namely, the state space \mathcal{S} is comprised of the set of all available

User and **Contextual** features in the ad marketplace data, the action space \mathcal{A} is made up of the set of available advertisements with the associated **advertisement** features and the reward would be the binary click label for each instance.

The aim of **Reinforcement Learning** is to interact with the MDP process environment in such a way that allows the agent to learn the *optimal policy* - i.e. the state-stage \rightarrow action mapping that maximizes the *value* over the longer term. We refine some of these terms with more definitions from (Pike-Burke, 2024b) below:

Definition 3.1.2. A **policy** $\pi = \{\pi_h\}_{h=1}^H$ is a sequence of mappings $\pi_h : \mathcal{S} \rightarrow \mathcal{A}$ for any $s \in \mathcal{S}, a \in \mathcal{A}$.

Definition 3.1.3. the **value** of a policy π from state $s \in \mathcal{S}$ in stage $h \in \{1, \dots, H\}$ is given by:

$$V_h^\pi = \mathbb{E} \left[\sum_{l=h}^H \gamma^{l-h} r_l(s_l, a_l) \mid s_h = s, a_l = \pi(s_l), s_{l+1} \sim P_l(\cdot | s_l, a_l) \right] \quad (3.1)$$

Where γ represents a chosen *discount factor* for potential rewards received in the future. The *optimal policy* π^* is then the one with the highest value, i.e.:

$$\pi_h^*(s) = \arg \max_{\pi \in \Pi} V_h^\pi(s)$$

for any $s \in \mathcal{S}$ and any $h \in \{1, \dots, H\}$. In order to optimize for the policy that maximizes the expected value, we would need to consider the expected value of taking a specific action a at specific stage h and state s , for some given policy π . This is given by the **Q-function**, defined below in definition 3.1.4.

Definition 3.1.4. The **Q-function** associated with taking action $a \in \mathcal{A}$ from state $s \in \mathcal{S}$ at stage $h \in \{1, \dots, H\}$ under some given policy π is given by

$$Q_h^\pi(s, a) = \mathbb{E} \left[\sum_{l=h}^H \gamma^{l-h} r_l(s_l, a_l) \mid s_h = s, a_h = a, a_l = \pi(s_l), s_{l+1} \sim P_l(\cdot | s_l, a_l) \right] \quad (3.2)$$

The relationship between the value function V and the state action value function Q is summarized in the **Bellman equations**. For any policy π and for all h, s, a :

$$\begin{aligned} V_h^\pi(s) &= Q_h^\pi(s, \pi_h(s)) \\ Q_h^\pi(s, a) &= r_h(s, a) + \gamma \sum_{s' \in \mathcal{S}} P_h(s' | s, a) V_{h+1}^\pi(s') \\ V_{H+1}^\pi(s) &= 0 \end{aligned}$$

The above leads to the key equations that underpin Reinforcement Learning - the **Bellman Optimality equations**.

Proposition 3.1.5. If V^* satisfies the Bellman Optimality Equations, then for all h, a, s :

$$\begin{aligned} V_h^*(s) &= \max_{a \in \mathcal{A}} Q_h^*(s, a) \\ Q_h^*(s, a) &= r_h(s, a) + \gamma \sum_{s' \in \mathcal{S}} P_h(s'|s, a) V_{h+1}^*(s') \\ V_{H+1}^*(s) &= 0 \end{aligned}$$

The above implies that the optimal policy π^* is given by:

$$\pi_h^*(x) = \arg \max_{a \in \mathcal{A}} Q_h^*(s, a)$$

In other words, the optimal policy is found by maximizing the Q -function at each stage and state. The basic idea of this is implemented in the *Dynamic Programming* algorithm, shown below:

Algorithm 1 Dynammic Programming algorithm

Require: $P_h(s'|s, a)$ and $r_h(s, a)$ are known

- 1: Set $V_{H+1}^*(s) = 0$ for all $s \in \mathcal{S}$
 - 2: **for** $h = H, \dots, 1$ **do**
 - 3: Calculate $Q_h^*(s, a) = r_h(s, a) + \gamma \sum_{s' \in \mathcal{S}} P_h(s'|s, a) V_{h+1}^*(s')$
 - 4: Set $\pi_h^*(s) = \arg \max_{a \in \mathcal{A}} Q_h^*(s, a)$
 - 5: Define $V_h^*(s) = \max_{a \in \mathcal{A}} Q_h^*(s, a) = Q_h^*(s, \pi_h^*(s))$
 - 6: **end for**
-

Of course in practice, we more often than not do not know the transition probabilities and reward function of the environment. The aim of Reinforcement Learning is to define an algorithm that adequately manages the *exploration-exploitation trade off*. Ideally, actions should be chosen in such a way that simultaneously allows for the collection of sufficient datapoints for estimating the reward function and transition probabilities, while also minimizing the long term cumulative *regret* as much as possible.

Definition 3.1.6. Let K be the total number of episodes, π^* be the optimal policy and π_t be the policy chosen for episode t . The the cumulative regret over K episodes is given by

$$\mathcal{R}_T = \sum_{t=1}^K \mathbb{E} \left[V_1^{\pi^*}(s_{1,t}) - V_1^{\pi_t}(s_{1,t}) \right] \quad (3.3)$$

One possible approach for achieving this is through algorithms that explicitly model the transition probabilities P_h . Two popular methods for doing so are the Upper Confidence Bound for Reinforcement Learning (UCBRL) (Auer et al., 2008) and the Thompson Sampling algorithm for Reinforcement Learning (Pike-Burke, 2024a). In UCBRL, the transition probabilities are empirically estimated on the basis of observed feedback from the environment, whereas Thompson Sampling proceeds by maining a posterior categorical distribution with a Dirichelet conjugate prior, and then sampling the transition

function from the posterior.

3.2. Q-Learning and Deep Q-Learning

3.2.1. Q-Learning

A major drawback with both of the UCBRL and Thompson Sampling algorithms is that they both require the state transition model to be approximated and stored. This poses a serious practical issue in the case of Ad personalization, since as we have covered in section 2.1, Ad marketplace data tends to be extremely sparse once encoded. This means that in order to fully calculate the transition probabilities, one would need to account for a vast number of state-action-transition tuples, which is likely to be computationally unfeasible. In this section, we explore Q-learning, a subdomain of Reinforcement Learning that aims to learn the Q-function directly, and is therefore *model free*.

Q-learning was pioneered by Watkins (1989) as a model-free, and therefore computationally efficient method for solving RL problems that have a sparse state and action space. The basic Q-learning algorithm works by maintaining an estimate of the Q-function for every state-action pair, and selecting a policy that is greedy with respect to this estimate (Pike-Burke, 2024b). The Q-function estimate $\hat{Q}(s, a)$ is usually initialized with its value set to $\hat{Q}_h(s, a) = H$ for all $s \in \mathcal{S}, a \in \mathcal{A}$. In each stage, the algorithm proceeds by choosing the action that maximizes the $\hat{Q}_h(s, a)$, and observing the reward received $r_h(s, a)$ and the resulting state s' . Before the next stage, the $\hat{Q}_h(s, a)$ estimate is then updated to reflect the actual results observed. The steps for the basic Q-learning algorithm are shown in Algorithm 2

Algorithm 2 Basic Q-Learning Algorithm. Source: (Pike-Burke, 2024b)

```

1: Initialization:  $\hat{Q}_{h,0}(s, a) = H$  for all  $s \in \mathcal{S}, a \in \mathcal{A}, h \in \{1, \dots, H\}$ 
2: for episode  $t = 1, \dots, K$  do
3:   Observe  $s_{1,t}$ 
4:   for Stage  $h = 1, \dots, H$  do
5:     Select action  $a_{h,t} = \arg \max_{a \in \mathcal{A}} \hat{Q}_{h,t}(s_{h,t}, a)$  and update  $N_{h,t}(s_{h,t}, a_{h,t})$ 
6:     Observe  $s_{h+1,t}$  and  $r_{h,t}(s_{h,t}, a_{h,t})$ 
7:     for All  $(s, a, s')$  values do
8:       if  $(s, a, s') = (s_{h,t}, a_{h,t}, s_{h+1,t})$  then
9:         Update  $\hat{Q}_{h,t+1}(s, a) = (1 - \alpha_{h,t})\hat{Q}_{h,t}(s, a) + \alpha_{h,t}(r_{h,t}(s, a) +$ 
            $\gamma \arg \max_{a' \in \mathcal{A}} \hat{Q}_{h,t}(s', a'))$ 
10:        else
11:          Set  $\hat{Q}_{h,t+1}(s, a) = \hat{Q}_{h,t}(s, a)$ 
12:        end if
13:      end for
14:    end for
15: end for

```

The advantage of the Q-learning algorithm is that the estimates for unobserved values

remains the same, there is no additional computation that needs to take place. We only need to store $H \times |\mathcal{S}| \times |\mathcal{A}|$ unique estimates for $\hat{Q}(s, a)$, as opposed to $H \times |\mathcal{S}| \times |\mathcal{A}| \times |\mathcal{S}|$ transition probabilities, which significantly lowers the memory requirement (Pike-Burke, 2024b). Note that in Algorithm 2 the $\alpha_{h,t}$ parameter represents an *update step size* parameter, which usually depends inversely on $N_{h,t}(s_{h,t}, a_{h,t})$.

3.2.2. Deep Q-Learning

While the basic Q-Learning algorithm significantly decreases the computational requirement by removing the need to store the transition probability model, keeping track of Q-function values may still be prohibitive in the case where the state and action spaces are prohibitively sparse, as is the case in the Ad personalization domain. All of the aforementioned algorithms are designed for discrete state and action spaces with relatively small cardinalities, and the performance of these algorithms deteriorates for increased number of state-action combinations that need to be accounted for (Pike-Burke, 2024b). For sparse environments, it is therefore desirable to find a suitable *function approximator* $f_{\Theta} : \mathbb{R}^n \rightarrow \mathbb{R}$ for the Q-function that can estimate the value of the of a state-action pair on the basis of a set of input action-state features $\mathbf{x} \in \mathbb{R}^n$ and a set of learned parameters Θ . This means that rather than having to store $\hat{Q}(s, a)$ values for every state-action combination, we will only have to store the function parameters Θ , and assume that $\hat{Q}(s, a) = f_{\Theta}(\mathbf{x})$, thereby changing the memory requirement from $H \times |\mathcal{S}| \times |\mathcal{A}|$ to simply $|\Theta|$.

Mnih et al. (2015) proposed the Deep Q-Learning algorithm in which the Q-function is approximated using a Deep Neural Network called a *Deep Q-Network*. The full Deep Q-Learning algorithm is shown in Algorithm 3.

In the original paper, the Deep Q-learning Network (DQN) algorithm was initially proposed to find the optimal playing policies for 49 of the classic Atari 2600 games, where a given state would be represented by the game’s pixel values, the set of actions were possible joystick movements and button presses and the rewards were the number of points accumulated throughout the game. Mnih et al. (2015) due to the highly sequential nature of the state-action-reward data, using newly observed data to directly update the Q-function DNN approximator would result in significant instabilities due to autocorrelation of inputs (Mnih et al., 2015). It is for this reason that the following modifications made in algorithm 3 over and above basic Q-Learning:

- In order to minimize the risk posed by the sequential dependancies in the newly observed data, Deep Q-Learning model is trained by means of *experience replay*. Every new observation is stored in memory \mathbf{D} . In order to fit the model, a sample of *experience observations* $(\phi_j, a_j, r_j, \phi_{j+1})$ is sampled from \mathbf{D} uniformly at random, and is then used to train the model by means of gradient descent.
- Using the same model for selection and calculating the gradient descent targets (y_j) tends to lead to further model instability as the y_j values are overestimated (Mnih et al., 2015). To prevent this, a separate *target model* \hat{f} is used to calculate the y_j values.

Algorithm 3 Deep Q-Learning with Experience Replay. Source: (Mnih et al., 2015)

```

1: Initialize: Replay memory  $\mathbf{D}$  to capacity  $\mathbf{N}$ .
2: Initialize: Q-function approximator  $f_\theta$  with random weights  $\Theta$ .
3: Initialize: Set target action-value function  $\hat{f}_{\hat{\Theta}}$  with  $\hat{\Theta} = \Theta$ 
4: for Episode  $t = 1, \dots, K$  do
5:   Initialize state sequence  $s_1$  and preprocess the sequence  $\phi_1 = \phi(s_1)$ 
6:   for Stage  $h = 1, \dots, H$  do
7:     with probability  $\epsilon$  select a random action  $a_h$ , otherwise select action  $a_h =$ 
        $\arg \max_{a \in \mathcal{A}} f_\Theta(\phi_h, a)$ 
8:     Execute action  $a_h$  and observe reward  $r_h(s_h, a_h)$  and the next state  $s_{h+1}$ 
9:     Preprocess the features of the next state  $\phi_{h+1} = \phi(s_{h+1})$ 
10:    Store the transition  $(\phi_h, a_h, r_h, \phi_{h+1})$  in  $\mathbf{D}$ 
11:    Sample a random set of transitions  $(\phi_j, a_j, r_j, \phi_{j+1})$ 
12:    Set  $y_j = \begin{cases} r_j, & \text{if } j = H \\ r_j + \gamma \max_a \hat{f}_{\hat{\Theta}}(\phi_{j+1}, a), & \text{otherwise} \end{cases}$ 
13:    Perform gradient descent step on  $L(\Theta) = (y_j - f_\Theta(\phi_j, a_j))^2$  with respect to
        $\Theta$ 
14:    Every  $C$  steps reset the target action-value function  $\hat{f} = f$  by setting weights
        $\hat{\Theta} = \Theta$ 
15:   end for
16: end for

```

3.3. DRN: Deep Reinforcement Learning for News Recommendation

DRN (Zheng et al., 2018) is a Deep Q-Learning framework that has been adapted to do online news personalization. In this setting, the objective is for the agent to learn a policy for choosing the ideal list of news articles to display to each user upon request, in order to maximize the long term engagement of all users with the news website. In this context, the state space \mathcal{S} is defined by *User features* (user’s past click activity) and *Contextual Features* (time, week day, freshness of the news), the action set \mathcal{A} is defined by the features describing the news articles available at the time of the news request (headline, provider, ranking, entity name, category etc.) and the reward is a combination of user news article clicks, and a measure of user activeness on the site.

In order to adapt to this news personalization context, the DRN algorithm introduces a few new components to the standard Deep Q-Network (DQN) algorithm introduced by Mnih et al. (2015). Firstly, it defines the reward as a combination of **user clicks** and **user activeness**, as formulated in the equation below:

$$r_{total} = r_{click} + \beta r_{active} \quad (3.4)$$

Zheng et al. (2018) defines r_{active} to take real values in $[0, 1]$ according to how frequently the user has visited the news site recently before t_i . Specifically, r_{active} is calculated using

Survival Analysis (Ibrahim et al., 2001; Jing and Smola, 2017).

Secondly rather than applying the ϵ -greedy method for exploration as in Algorithm 3, DRN uses the **Dueling Bandit Gradient Descent** algorithm. This algorithm proceeds by generating an *explore network* $\tilde{Q}(s, a) \approx \tilde{f}_{\tilde{\Theta}}$ before each timestamp t_i .

Definition 3.3.1. The *explore network* $\tilde{f}_{\tilde{\Theta}}$ with weights $\tilde{\Theta}$ has the same architecture as the base Deep Q-Network $Q \approx f_{\Theta}$ (otherwise referred to as the *exploit network*), and the weights $\tilde{\Theta}$ are calculated as

$$\tilde{\Theta} = \Theta + \alpha U \Theta$$

where Θ represents the weights for Q , $U \sim \text{Uniform}(-1, 1)$ and α is an explore parameter

For each user-query session at each timestamp t_i , the list of news articles L_i is then chosen from the list of candidates I_i by randomly combining recommendations using both the exploit network Q and explore network \tilde{Q} . If the items recommended by \tilde{Q} receive better feedback from the user by the end of the session, the exploit network weights Θ are updated towards $\tilde{\Theta}$.

Lastly, the DRN algorithm uses the Double DQN target calculation to calculate y_t (replacing line 12 in algorithm 3)

$$y_j = \begin{cases} r_j, & \text{if } j = H \\ r_j + \gamma \hat{f}_{\tilde{\Theta}}(\phi_{j+1}, \arg \max_a f_{\Theta}(\phi_{j+1}, a)), & \text{otherwise} \end{cases} \quad (3.5)$$

The key distinction in the equation above is that rather than using the target network $\hat{f}_{\tilde{\Theta}}$ to directly estimate the value of future rewards $Q(\phi_{j+1}, a_{j+1})$, the base Q-function approximator f_{Θ} is used to find the optimal action at time $j + 1$, after which the target approximator $\hat{f}_{\tilde{\Theta}}$ is used to evaluate the future value of this action. This method was introduced by van Hasselt et al. (2016) in order to mitigate instabilities in the DQN algorithm.

The DRN algorithm is composed of an Offline part and an Online part, as shown in Figure 3.1. The Offline part consists fitting the initial Q-function approximator network f_{Θ} , using previously collected session records containing the user, contextual and news article features previously discussed. The Online Learning part of the DRN framework proceeds as follows, as per (Zheng et al., 2018):

1. **Push:** At each timestamp t_i , a user u browses to the news website, thereby submitting a request for news articles. The agent G takes account of the user and context features, as well as the features for the set of currently available news candidates I_i . The agent then selects the top l candidates. The list of L_i candidates is compiled by mixing items recommended by the *exploit Q-network* Q and the *explore network* \tilde{Q} . The list is then shown to the user.
2. **Feedback:** The user will then provide feedback by either clicking or not clicking on each of the L news articles. This feedback is stored in memory D , along with updated user activeness metrics for user u .

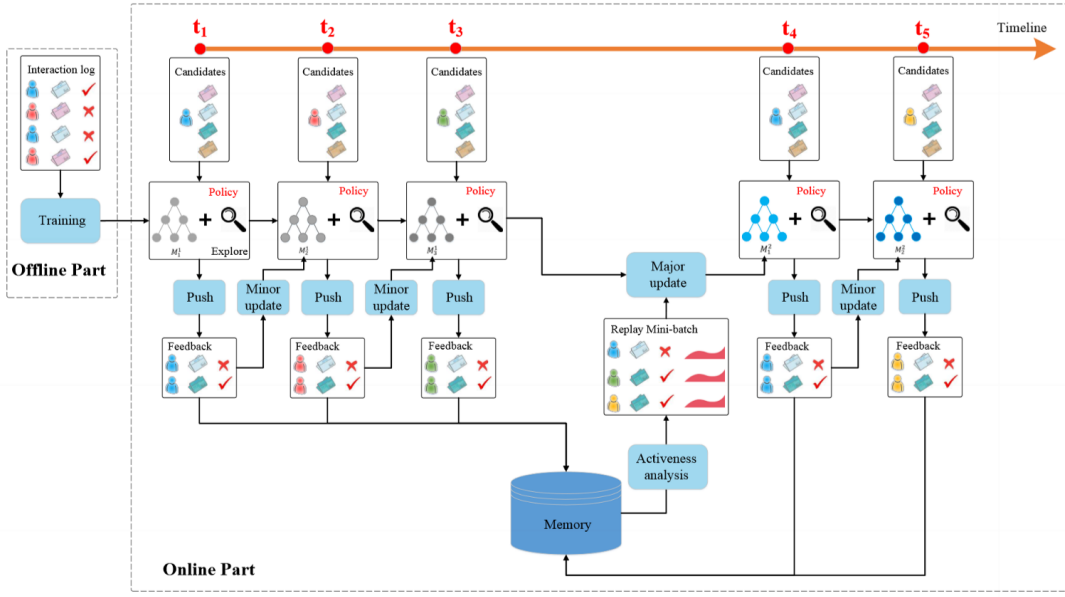


Figure 3.1.: DRN Framework. Source: (Zheng et al., 2018)

3. **Minor Update:** After each timestamp t_i , the agent collects the user's feedback, and compares the relative CTR performance of news candidates recommended by Q and \hat{Q} . If \hat{Q} outperformed Q , then the weights of the explore network W are updated to those of the explore network \tilde{W} . Otherwise the weights of the exploit network remain unchanged.
4. **Major Update:** After a pre-defined time period T_R , the agent will use the feedback data stored in D to update the exploit network Q . The reward will be based on a compination of user clicks and activeness, and Q will be updated using the Experience Replay technique from Algorithm 3, with the target value adaptation from equation 3.5.

4. Deep CTR model Evaluation

As explained in the preceeding introduction, chapter 4 is dedicated for evaluating a range of different click prediction models. The intention is then to incorporate the best model candidate in a Deep Reinforcement Learning framework for Ad personalization in chapter 5. The contents of chapter 4 include the results of two successive experiments:

1. A **Comparitive Model Analysis**, whereby the predictive performance of a range of different CTR models is measured using equivalent hyperparameter settings and the same benchmark CTR datasets.

Research Question: *Which of the CTR prediction models in scope have the highest predicted performance when measured using equivalent hyperparameter settings and using the same benchmark CTR prediction datasets?*

2. A **Hyperparameter Setting Analysis**, whereby we take the highest performing model from the previous experiment above, and calculate and compare that model's predictive performance for different parameter settings. To simplify the complexity of this task, each chosen parameter was set to to a finite set of values, and this was conducted sequentially for the different parameters. This will be explained in more detial in section 4.2.4.

Research Question: *What are the ideal hyperparameter values for the given CTR prediction model?*

We first proceed by explaining the model selection criterea and listing the candidate models in section 4.1. We then describe the Experiment Setup for the model evaluations in section 4.2, including data preprocessing, evaluation metrics, optimization algorithms and hyperparameter selection. Finally, we conclude the chapter by presenting the results for the experiments above in section 4.3, in which the **Deep and Cross Network** (DCN) architecture (Wang et al., 2017) was revealed to have the highest predictive accuracy on our chosen datasets.

4.1. Models and Model selection Criteria

DeepCTR classification is an extremely active field of research, with many different model architectures being explored by different authors. It is because of this reason that it is practically impossible to evaluate all models within the scope of this project. For the purposes of this paper, the scope of models has therefore been narrowed down using the following model selection criteria:

- Competitive prediction accuracy in the KDD12, Criteo and Avazu datasets as published on Papers with Code (Meta AI Research, 2024).
- Ideally, I was looking for a representative set of models for each model type as discussed in (Zhang et. al. 2021). Therefore I was looking for models that employed Product Interaction Operators, Attention Operators and Factorization Machines as a basis.
- The code for the model has to be accessible and intuitive to use. To implement the experiments in this chapter, I made use of the DeepCTR Python package (Shen, 2017).

On the basis of the above criteria, the following models from chapter ?? have been selected for the scope of this paper:

- Factorization Supported Neural Networks (FNN) (Zhang et al., 2016)
- Product Based Neural Networks (PNN) (Qu et al., 2016)
- Neural Factorization Machines (NFM) (He and Chua, 2017)
- Deep and Cross Network (DCN) (Wang et al., 2017)
- Wide and Deep Learning (WDL) (Cheng et al., 2016)
- DeepFM (DFM) (Guo et al., 2017)
- Automatic Feature Interaction (AutoInt) (Song et al., 2019)
- Convolutional Click Prediction Model (CCPM) (Liu et al., 2015)
- Feature Generation by Convolutional Neural Network (FGCNN) (Liu et al., 2019)

For comparison, we also evaluate the predictive performance of the shallow models, as a baseline:

- Logistic Regression (LR) (Richardson et al., 2007)
- 2-way Factorization Machines (FM) (Rendle, 2010)

4.2. Experiment Setting

The full script for both experiments outlined above is contained in the iPython notebook `ctr_model_testing.ipynb`, which is available on the Github Repository for this project (Batěk, 2024). All experiments were carried out using Tensorflow version 2.14 on AWS Sagemaker JupyterLab, utilizing a ml.g5.2x.large compute instance. Model implementations from the DeepCTR Python package (Shen, 2017) were used for all Deep models. For full Python environment specifications, please refer to the `environment_gpu.yml` file on the aforementioned Github repository for this project.

4.2.1. Datasets and Preprocessing

In order to evaluate and compare the predictive performance of each of the previously mentioned models, we perform experiments using three widely known real-world benchmark datasets for click-through rate prediction.

KDD12

The **KDD12** dataset was first released for the KDD12 cup 2012 competition (Aden, 2012), with the original task being to predict the click through rate for a given number of impressions - i.e. the ratio of ad impressions that would ultimately result in a click. Each line represents a training instance derived from the session logs for the advertizing marketplace. In the context of this dataset, a “session” refers to an interaction between a user and the search engine, containing the following components; the user, a list of adverts returned by the search engine and shown (impressed) to the user and zero or more adverts clicked on by the user. Each line in the training set includes, Click and Impression counts, Session features, User features and Ad features.

Avazu

The **Avazu** dataset was originally released in 2014 for a CTR prediction Competition on Kaggle (Wang and Cukierski, 2014). The data is composed of 11 days worth mobile ad marketplace data. Much like the KDD12 dataset above, this dataset contains features ranging from user activity (clicks), user identification (device type, IP) to ad features.

Criteo

Finally, the **Criteo** dataset is another benchmark CTR prediction dataset that was originally released on Kaggle for a CTR prediction competition (Tien et al., 2014). The original dataset is made up of 45 Million user’s click activity, and contains the click/no-click target along with 26 categorical feature fields and 13 numerical feature fields. Unlike the other two datasets however, the semantic significance of these fields is not given - they are simply labelled as “Categorical 1-26” and “Numerical 1-13” respectively.

Exploratory Data Analysis and Preprocessing

The KDD12, Avazu and Criteo datasets mentioned above contain approximately 150, 231 and 99 million records, adding up to a 26.2 GB collective memory requirement. As a first step in preprocessing, each dataset was shuffled and split into training (80%) and validation (20%) sets. The size of the datasets necessitated the use of Amazon Web Services’ Data Wrangler Tool (Amazon Web Services, 2024) for shuffling and splitting, and this was done using a random seed of 42. In order to restrict the training time and cost for the 11 models to a reasonable amount (approximately half a minute on average per epoch), model fitting was conducted using a 157440 record training subsample and a 39360 record subsample of each dataset.

We then proceeded to preprocess the categorical and numerical features. As previously discussed in chapter ??, ad platform categorical features tend to contain a lot of unique values per feature - i.e. they exhibit high cardinality.

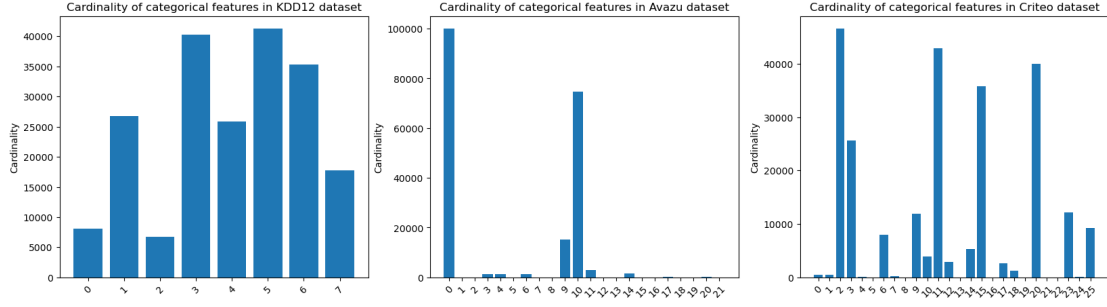


Figure 4.1.: Categorical feature cardinalities from subsets of each dataset

A common remedy to the above issue is to *bin* the categorical feature values before one-hot encoding or embedding, according to some given threshold (Song et al., 2019). This essentially means that for a given threshold t , we retain only the values for the multi-value categorical features that have more than t occurrences in the dataset. As recommended by Song et al. (2019), the binning thresholds were set such that $t = 10, 5, 10$ for Criteo, KDD12 and Avazu respectively. The categorical feature values were then label encoded as integers in descending order according to the appearance of each value in the dataset, with integer keys starting at 1. In otherwords, the most frequent value mapped to 1, the second most frequent to 2, and so on. The 0 key was reserved for either infrequent or unknown categorical feature values.

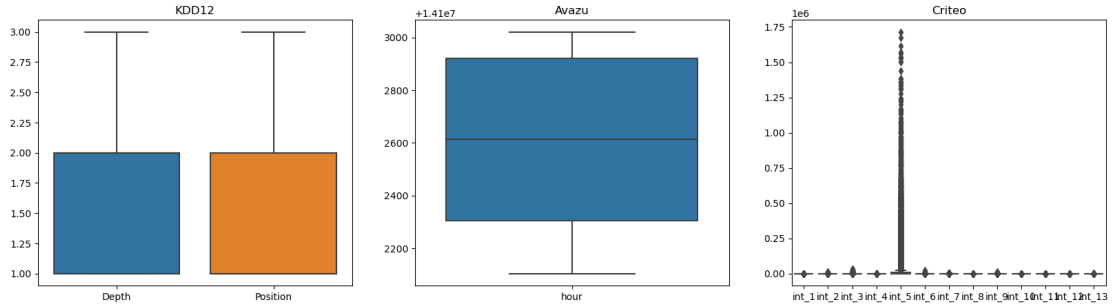


Figure 4.2.: Boxplots of numerical features in the datasets

Subsequently, an examination of the boxplots (see figure 4.2) for the numerical features in each of the datasets reveals the presence of high variance numerical outliers, particularly in the case of the Criteo dataset. In order to ensure efficient training by means of gradient descent, these values needed to be normalized to unit variance and zero mean. In other words, for each numerical feature x , the following transformation

was applied:

$$z = \frac{x - \bar{x}}{\sigma}$$

where \bar{x} and σ represents the mean and standard deviation of the the numerical feature in question. Furthermore, for the Criteo Dataset the following transformation was applied to the normalized values, as recommended by Song et al. (2019):

$$\tilde{z} = \begin{cases} z & \text{if } z \leq 2 \\ \log^2(z) & \text{otherwise} \end{cases}$$

Finally, since the datasets will be used to train a binary classifier, we examined the distributions of target label values in each of the datasets. In Figure 4.3, we see that there is a significant target-variable imbalance for all three datasets, with positive label rates ranging from 5% for KDD12 to 25% for Criteo. This range is fairly typical of what one can expect of average digital ad placement Click-Through rates, and KDD12 is the most representative of the three in this regard (CXL). We can expect that this imbalance will have an adverse impact model Precision and AUC. Due to the large imbalance for KDD12, we upweight all positive class labels by a factor of 4.98 and downweight all of the negative labels by a factor of 0.26. in all experiments.



Figure 4.3.: Target variable distribution from 10K record random samples from each dataset

4.2.2. Evaluation Metrics

Predictive performance of each model was assessed in terms of the following five metrics:

- **Binary Cross Entropy Loss:** Also known as logarithmic loss. This metric penalizes the model when the predicted log likelihood of a positive label $\hat{y} = \sigma(f_{\Theta}(\mathbf{x}))$ deviates from the log likelihood that $y = 1$ as suggested by the data. For

K feature-label observations, this Loss metric is calculated as:

$$L^{\text{Cross-Entropy}}(\mathbf{x}, y, \Theta) = - \sum_{k=1}^K [y \log \sigma(f_{\Theta}(\mathbf{x})) + (1 - y) \log (1 - \sigma(f_{\Theta}(\mathbf{x})))]$$

Binary Cross Entropy is commonly used as a loss metric in multiple binary classification models (Zhang et al., 2021), and has therefore been utilized as the primary loss function for model training for all experiments in this report.

- **AUC:** Area under ROC curve is another commonly used metric for binary classification, and it has been validated as a good evaluation metric for the Click Through Rate prediction task (Graepel et al., 2010).
- **Binary Accuracy:** Binary Accuracy measures the percentage of times that the predicted label (with regards to the positive label likelihood prediction \hat{y} and some likelihood threshold $t \in (0, 1)$) matches the actual label y for a set of K observations.

Let

$$g_t(\hat{y}) = \begin{cases} 1 & \text{if } \hat{y} \geq t \\ 0 & \text{otherwise} \end{cases}$$

and let \mathbb{I} be the indicator function where $\mathbb{I}_a(b) = 1$ if $a = b$ and $\mathbb{I}_a(b) = 0$ otherwise. Then

$$M^{\text{Binary Accuracy}}(\mathbf{x}, y, \Theta, t) = \frac{\sum_{k=1}^K \mathbb{I}_{y_k}(g_t(\sigma(f_{\Theta}(\mathbf{x}_k))))}{K}$$

Binary Accuracy is an intuitive metric to understand, since it simply shows how often the model is correct. However, this can be misleading in cases where label imbalance is prevalent, and it therefore often prudent to also refer to the Precision and Recall metrics. For the experiments in this report, we evaluate the models using Binary Accuracy with $t = 0.5$.

- **Precision:** Precision measures the ratio of observations with positive predicted labels that in fact have positive labels in the data:

$$M^{\text{Precision}}(\mathbf{x}, y, \Theta, t) = \frac{\sum_{k=1}^K \mathbb{I}_{y_k}(g_t(\hat{y}_k)) \cdot \mathbb{I}_1(g_t(\hat{y}_k))}{\sum_{k=1}^K \mathbb{I}_1(g_t(\hat{y}_k))}$$

Where $\hat{y}_k = \sigma(f_{\Theta}(\mathbf{x}_k))$. In the context of Ad personalization, the Precision metric can be seen as an indicator of quality of the set of Ads retrieved for the user, from the perspective of that user's Ad preferences. Like in the case of Binary Accuracy, we evaluate the models in this report using Precision with $t = 0.5$

- **Recall:** Recall measures the proportion of the data observations with true positive labels that have positive predicted labels:

$$M^{\text{Recall}}(\mathbf{x}, y, \Theta, t) = \frac{\sum_{k=1}^K \mathbb{I}_{y_k}(g_t(\hat{y}_k)) \cdot \mathbb{I}_{y_k}(1)}{\sum_{k=1}^K \mathbb{I}_{y_k}(1)}$$

The Recall Metric is relevant in the Ad personalization context, since it in essence reveals how good the model is at finding Ads that the user will click on. Again, in this report we set the predicted probability threshold t to 0.5.

4.2.3. Optimization Algorithms

In section 4.2.2 we have already stated that the primary loss function used in this report for model fitting is the Binary Crossentropy Loss function. For Logistic Regression (LR) and Factorization Machines (FM), the Stochastic Gradient Descent algorithm (Robbins and Monro, 1951) was used to optimize the model weights, as recommended in the original papers (Rendle, 2010; Richardson et al., 2007). For the DNN models, we used the Adam Optimizer (Kingma and Ba, 2014), a widely popular optimization algorithm for training Deep Neural Networks. In both cases, we set the learning parameter to $\eta = 0.001$, which is the standard learning rate setting for the Keras Adam Optimizer implementation (Chollet et al., 2023).

In order to ensure that training times (and therefore training cost) remained within a reasonable range, all models were trained to a maximum of 15 epochs. In addition to this, the Keras EarlyStopping Callback was used with `patience` parameter set to 5 epochs. This was done to further ensure that training time remained within a reasonable range, as well as in order to prevent model fitting.

4.2.4. Hyperparameter Selection

As mentioned at the beginning of section 4.2, the DeepCTR Python model developed by Shen (2017) was leveraged to implement all the Deep CTR models listed in section 4.1. The majority of the of the model classes in the DeepCTR package use the following hyperparameter inputs, which we have standardized for experiment 1:

- **DNN Hidden Units:** This parameter controls the number of hidden layers and the number of neurons in each hidden layer of the MLP component of the model. For experiment 1, this parameter was set to [200, 200, 200] for all models - i.e. 3 layers, containing 200 neurons each.
- **DNN Dropout Likelihood:** For every neuron in the MLP components in the model, the DNN Dropout parameter controls the likelihood that the neuron is removed during training. Srivastava et al. (2014) found that introducing such randomness during training can greatly improve regularization. As recommended by Guo et al. (2017), this parameter was set to 0.6 for both experiments.
- **Categorical Feature Embedding Dimension:** This is represented by variable D in equation 2.3. For all experiments, we set $D = 4$.

- **Embedding L2 Regularization:** The L2 regularization strength that was applied while fitting the categorical feature embedding matrices (B_i). This was set to 0.005 for both experiments.
- **Linear L2 Regularization:** The L2 regularization strength that was applied in the linear component of the model, such as the Wide component of the WDL model. For relevant models, this was set to 0.005 for both experiments.
- **DNN L2 Regularization:** The L2 regularization strength that was applied in the MLP component of the model, such as the Deep component of the WDL model. For relevant models, this was set to 0.005 for both experiments.
- **DNN Batch Normalization:** This parameter controls whether the internal activation values of the MLP component are normalized for every batch during training, so as to promote training stability and introduce an additional regularization effect (Ioffe, 2015). This parameter was set to *True* for all models and experiments.

In experiment 1, all models were compiled and fitted with the standard hyperparameter settings mentioned above. In experiment 2, we took inspiration from (Guo et al., 2017), and explored the predictive accuracy of the best performing model from experiment 1 for different *DNN Hidden Unit* settings, namely sequentially cumulatively the following aspects:

1. **Neurons per layer:** Here we scored the model when using 100, 200, 300, 400 and 500 neurons per layer in the MLP component. Tests were carried out using 3 hidden layers.
2. **Number of layers:** Here we scored the model when using 2, 3, 4, 5 and 6 hidden layers in the MLP component. Tests were carried out using 200 neurons per layer.
3. **DNN shape:** Here we compared the predictive performance for different shapes of the Deep Neural Network, namely constant, increasing, decreasing, and diamond.

Note that experiment 2 was conducted *cumulatively* in the order above. This means that the best Neuron per layer setting was determined first and that this setting was used when exploring the Layer count settings, and so on. Since experiment 1 revealed that the DCN model was the best performing candidate, we additionally elected to explore the performance of this model for different cross layer parameter values, namely $c \in \{2, 3, 4, 5, 6\}$.

4.3. Deep CTR Model Results and Discussion

4.3.1. Experiment 1: Comparative Model Analysis

The results for experiment 1 for the KDD12, Avazu and Criteo datasets are shown in tables 4.1, 4.2 and 4.3 respectively. A visualization of these results has been included in

Model	Epochs	Log Loss	Accuracy	Precision	Recall	AUC
LR	14	0.6081	0.7647	0.0669	0.3671	0.6372
FM	14	0.6581	0.5911	0.0604	0.618	0.6272
FNN	0	0.5607	0.7356	0.0718	0.4584	0.6544
PNN	6	0.5804	0.9591	0.0	0.0	0.5874
WDL	3	0.5653	0.7204	0.0723	0.4932	0.6637
DFM	2	0.5826	0.6684	0.0664	0.5441	0.6646
AUTOINT	10	0.2667	0.926	0.0911	0.0901	0.6038
FGCNN	14	0.5706	0.7134	0.0751	0.5311	0.6715
NFM	14	0.4142	0.8582	0.1082	0.3404	0.6903
DCN	13	0.415	0.853	0.1048	0.3441	0.694
CCPM	10	0.5911	0.6815	0.0586	0.4509	0.5945

Table 4.1.: Experiment 1 model scores on KDD12 dataset

Model	Epochs	Log Loss	Accuracy	Precision	Recall	AUC
LR	14	0.4208	0.8334	0.5824	0.0081	0.682
FM	14	0.4167	0.8339	0.5636	0.0249	0.6946
FNN	14	0.421	0.833	0.5	0.0002	0.6865
PNN	6	0.4511	0.833	0.0	0.0	0.5
WDL	14	0.421	0.833	1.0	0.0002	0.6867
DFM	14	0.4052	0.8339	0.59	0.0179	0.7249
AUTOINT	3	0.4031	0.8355	0.5645	0.0653	0.7278
FGCNN	3	0.4066	0.833	0.5	0.0005	0.7221
NFM	6	0.402	0.836	0.5928	0.0578	0.7303
DCN	13	0.4011	0.8359	0.5699	0.072	0.7327
CCPM	13	0.4044	0.833	0.0	0.0	0.7293

Table 4.2.: Experiment 1 model scores on Avazu dataset

the appendix in Figure A.1. Only the metrics for the epochs with the minimum achieved training loss function (Binary Crossentropy) are reported. The first column in the tables indicates the epochs in which the minimum loss function value was attained. Recall that in each case, the models were fitted to a maximum of 15 epochs, with an EarlyStopping callback and a patience value set to 5 epochs.

We see that our models generally did not reach the levels of predictive performance mentioned in the respective experiments conducted in the original papers. As an example of this, DeepFM and DCN attained a minimum Binary Crossentropy of 0.45083 and 0.4419 as reported in (Guo et al., 2017) and (Wang et al., 2017), but in our experiments these models attained minimum Log Loss values of 0.5546 and 0.5225 respectively. This can be expected, since the fact that the intention of experiment 1 was to deliver a broader comparative analysis of a larger number of models, we have had to use a relatively small subsamples of the benchmark datasets. The original authors of the models were generally

Model	Epochs	Log Loss	Accuracy	Precision	Recall	AUC
LR	14	0.5675	0.7135	0.6283	0.2378	0.7058
FM	14	0.5627	0.7178	0.6367	0.2575	0.7128
FNN	14	0.5645	0.714	0.6519	0.2117	0.7133
PNN	14	0.5663	0.7203	0.6377	0.2745	0.7125
WDL	14	0.5645	0.7139	0.6522	0.2108	0.7132
DFM	3	0.5546	0.7225	0.662	0.2567	0.7252
AUTOINT	1	0.5467	0.7303	0.6517	0.3227	0.7366
FGCNN	4	0.5646	0.7139	0.6494	0.214	0.7131
NFM	3	0.5309	0.7392	0.6489	0.3878	0.7575
DCN	11	0.5225	0.7442	0.6476	0.4254	0.7673
CCPM	3	0.59	0.6897	0.5796	0.0808	0.6692

Table 4.3.: Experiment 1 model scores on Criteo dataset

not constrained in this way, and had therefore used larger samples; for Deep & Cross Learning, Wang et al. (2017) used 41 million records of the Criteo dataset, and were therefore able to reach much higher levels of predictive performance.

When comparing the performance of SHallow models to their Deep counterparts, we find that although the Logistic Regression and Factorization Machines models are consistently in the bottom 5 models in terms Binary Crossentropy and AUC for the three datasets, the difference in performance is not significantly large, and in some cases they outperformed some of the Deep models (such as in the case of WDL and PNN for the Avazu dataset). This marginal performance differential consistent with what has been shown with experiments using larger dataset samples in (Guo et al., 2017; Liu et al., 2019; Wang et al., 2017), and shows that although DNN models do tend to perform better, LR and FM can still be considered to be viable “parameter-light” alternatives to DNN models in CTR prediction.

The results shown reveal that the **Deep and Cross Network** (DCN) model outperformed the rest relatively consistently for all three datasets. For both Avazu and Criteo, DCN outperformed all other models on the basis of both Binary Crossentropy and AUC, whereas for the KDD12 dataset it outperformed in terms of AUC. The DCN model also performed relatively well in terms of both Precision and Recall, scoring on par with or better than the majority of the models in scope. It displayed a significant degree of efficiency during training, with relatively stable improvements in loss for successive epochs (this is where the closest contender, NFM, struggled - particularly with the Criteo and Avazu datasets). It is for these reasons that the DCN model was selected as the model for use in experiment 2 and in chapter 5.

There are several limitations of the method that we employ in experiment 1. We already mentioned that due to the fact that we are using relatively small subsamples of the three datasets, we do not attain the stated Log Loss and AUC from the original papers. Secondly, as we elected to standardize the DNN hyperparameter settings as described in section 4.2.4 and to keep all hyperparameter values as per the defaults in

the DeepCTR package (Shen, 2017), it is possible that this may have resulted in sub-optimal hyperparameter settings for the specific models. The final notable limitation stems from the target variable imbalance mentioned in section 4.2.1. Such target label imbalance makes it difficult for the model to learn which feature combinations are most associated with a positive label, since the number of positively labelled observations is limited. In the case of KDD12 where the class imbalance is most severe, we partially remedy this by applying class weights during training. Unfortunately, this method tends to result in training instability. Some of the DeepCTR researchers such as Liu et al. (2019) used negative sampling to remedy the class imbalance issue instead.

4.3.2. Experiment 2: Hyperparameter Setting Analysis

Experiment 1 revealed that the DCN model consistently outperformed all of the models in scope for the data and standard parameter settings discussed in section 4.2. In experiment 2 we sequentially explore each of the hyperparameter settings as discussed in the latter half of section 4.2.4, by refitting the DCN model to each hyperparameter setting. This hyperparameter experiment was inspired by a similar exercise conducted in section 3.3 of (Guo et al., 2017). Experiment 2 was conducted using the KDD12 dataset samples only.

Neurons per Layer

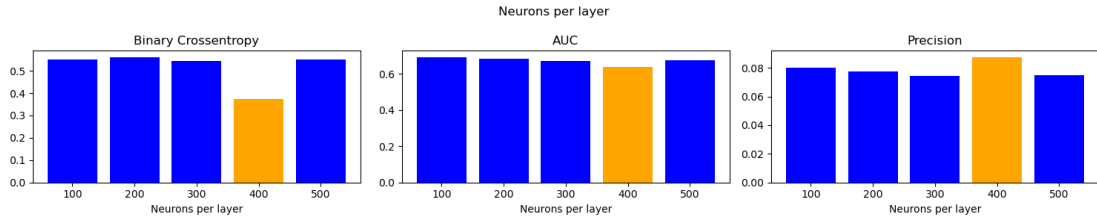


Figure 4.4.: Model scores for different neuron counts

When all other factors remain the same, increasing the number of neurons per layer introduces complexity in the model (Wang et al., 2017). The level of expressiveness that this brings initially improves the degree to which the model can learn and generalize more complex patterns in the data, but will eventually result in overfitting for higher neuron values. Figure 4.4 reveals that for the DCN model, the best Binary Crossentropy and Precision scores were attained with 400 neurons per layer.

Number of Layers

Similarly as to the case with neurons, we find that the same model bias-variance dynamic applies when exploring the performance for an increasing number of layers. Figure 4.5 reveals that initially, the Binary Crossentropy and Precision of the DCN model improved

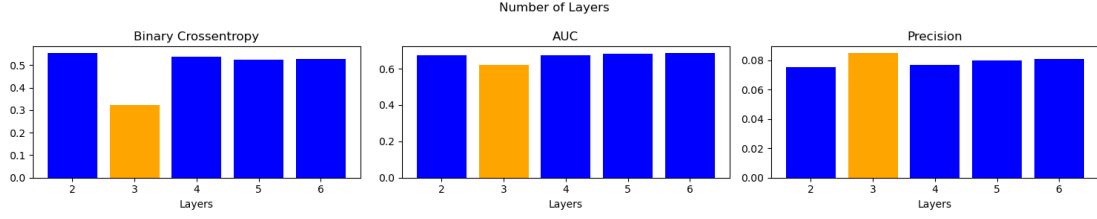


Figure 4.5.: Model scores for different layer counts

from 2 to 3 layers, but performance deteriorated in terms of both of these metrics thereafter. The DCN model therefore performed best with 3 layers.

DNN Shape

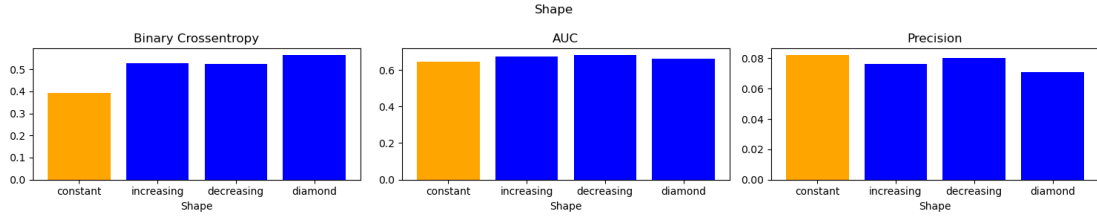


Figure 4.6.: Model scores for different DNN shapes

For shape exploration, we fix the total number of neurons and the number of layers to 1200 and 3 respectively in order to remain in line with the two previous findings. This means that in terms of DNN Neuron settings, we used $[400, 400, 400]$ for Constant, $[300, 400, 500]$ for Increasing, $[500, 400, 300]$ for Decreasing and $[300, 600, 300]$ for Diamond. Figure 4.6 revealed that Constant yielded the best results for the DCN model.

Number of Cross Layers

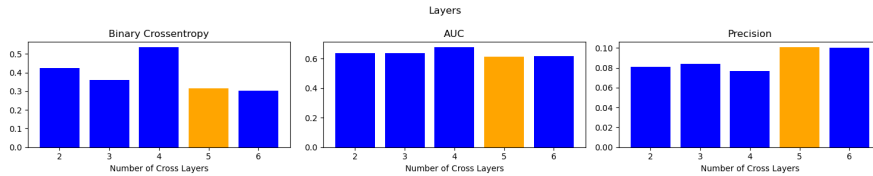


Figure 4.7.: Model scores for different Cross Layer settings

Finally, we explore the DCN model performance for different Cross Layer settings, ranging from 2 to 6 Cross Layers. Recall from section 2.6 that the Cross Network component in the DCN model explicitly captures feature interactions up to order $k + 1$,

where k is the number of Cross Layers. In Figure 4.7, we see that the DCN model generally tends to perform better for higher Cross Layer parameter values. We choose to set this parameter to 5, as informed by the Precision metric specifically. The final model and parameter settings chosen after experiments 1 and 2 are shown in table 4.4.

Hyperparameter	Value
Model	DCN
Neurons per Layer	400
Number of Layers	3
DNN Shape	Constant
Number of Cross Layers	5

Table 4.4.: Model and Hyperparameters chosen after experiments 1 and 2

Experiment 2 shares the same limitations stemming from the small data sample size and target variable imbalance as mentioned for experiment 1. In addition, due to training time limitations we have had to employ the sequential parameter search method described above, which would not explore all of the possible parameter combinations, as in the case of a full Grid Search. This entails that the parameters found in experiment 2 are not guaranteed to be optimal.

5. Deep Reinforcement Learning for Ad Personalization

In chapter 4, we conducted experiments to ascertain the best performing candidate CTR prediction model out of those listed in section 4.1, and to determine the ideal hyperparameter values. As a result we found the DCN model to be the ideal candidate. In chapter 5 we propose the Deep Reinforcement Learning for Ad Personalization (DRL-AP) algorithm, a Reinforcement Learning algorithm that leverages the DCN model as a Deep Q-Network function approximator, and is otherwise largely based in DRN algorithm. We then conduct an offline simulation using the KDD12 dataset introduced in chapter 4 as a proof-of-concept for DRL-AP.

5.1. DRL-AP Algorithm

The DRL-AP algorithm is largely based on the DRN algorithm described in section 3.3, and leverages the DCN model as the Q-function approximator. Since the DCN model trained in chapter 4 is trained as a binary classifier, the target value used during the experience replay update y_j can only take values on the interval $[0, 1]$. Therefore, we modified the target value label calculation in equation 3.5 to the following:

$$y_j = \begin{cases} r_j, & \text{if } j = H \\ \frac{1}{1+\gamma} \left(r_j + \gamma \hat{f}_{\hat{\Theta}}(\phi_{j+1}, \arg \max_a f_{\Theta}(\phi_{j+1}, a)) \right) & \text{otherwise} \end{cases} \quad (5.1)$$

thereby normalizing the target value by a factor of $1 + \gamma$ for sequences where $j \neq H$. Furthermore, due to the fact that we have been constrained to offline testing only for this project, we have chosen not to include the user activeness component from DRN in DRL-AP. However, this can straightforwardly be included in future iterations. The DRL-AP algorithm is summarized in 4. In the ad personalization context, the state space \mathcal{S} is defined as by the user and contextual features at time t , the action set \mathcal{A}_t is defined by the ad's available for display at time t and the rewards are the user clicks.

5.2. Experiment Setting

To provide a proof-of-concept for the DRL-AP algorithm, we conduct a simulation of the online learning environment using the KDD12 dataset. The pretraining step of the DRL-AP algorithm is implemented in the Python Notebook `rl_model_pretraining.ipynb`, whereas the simulation of the Online Part of the algorithm using the KDD12 dataset is

Algorithm 4 Deep Reinforcement Learning for Ad Personalization Algorithm

```

1: Pretrain: DCN Q-function approximator  $f_\theta$  with offline historical data.
2: Initialize: Replay memory  $\mathbf{D}$  to capacity  $\mathbf{N}$ .
3: Initialize: Set target action-value function  $\hat{f}_{\hat{\Theta}}$  with  $\hat{\Theta} = \Theta$ 
4: for Episode  $k = 1, \dots, K$  do
5:   for Session  $t = 1, \dots, M$  do
6:     Observe state  $s_{(t-1)P+1}$  as a combination of user  $u$  and context/query  $c$  features
7:     Preprocess and set state values for all positions in the ad list  $\{\phi_h\}_{h=(t-1)P+1}^{tP} = \phi(s_{(t-1)P+1})$ 
8:     Retrieve the list of available ads on the platform  $\mathcal{A}_t$ 
9:     Initialize: Ranked ad List  $L_t$  of length  $P$  to display to the user
10:    Initialize: Explore model weights  $\tilde{\Theta} = \Theta + \alpha U(-1, 1)\Theta$ 
11:    Initialize: Explore model  $\tilde{f}_{\tilde{\Theta}}$ 
12:    for List position  $p = 1, \dots, P$  do
13:       $h = (t-1)P + p$ 
14:      with probability  $\epsilon$  select ad  $a_h = \arg \max_{a \in \mathcal{A}_t} \tilde{f}_{\tilde{\Theta}}(\phi_h, a)$ , otherwise select
      ad  $a_h = \arg \max_{a \in \mathcal{A}_t} f_\Theta(\phi_h, a)$ 
15:      Place ad  $a_h$  in position  $p$  of the ad list  $L_t$ 
16:      Remove ad  $a_h$  from  $\mathcal{A}_t$  for the remainder of the session
17:    end for
18:    PUSH: Display list  $L_t$  to the user
19:    FEEDBACK: Receive clicks feedback  $\{r_h\}_{h=(t-1)P+1}^{tP}$  from user
20:    if Session CTR for  $\tilde{f}_{\tilde{\Theta}}$  exceeds Session CTR for  $f_\theta$  then
21:      MINOR UPDATE Update  $\Theta$  to  $\tilde{\Theta}$ 
22:    end if
23:    Store the transitions  $(\phi_h, a_h, r_h, \phi_{h+1})$  in  $\mathbf{D}$ 
24:  end for
25:  Sample a random set of transitions  $(\phi_j, a_j, r_j, \phi_{j+1})$  from  $\mathbf{D}$ 
26:  Set  $y_j = \begin{cases} r_j, & \text{if } j = M \cdot P \\ \frac{1}{1+\gamma} \left( r_j + \gamma \hat{f}_{\tilde{\Theta}}(\phi_{j+1}, \arg \max_a f_\Theta(\phi_{j+1}, a)) \right) & \text{otherwise} \end{cases}$ 
27:  MAJOR UPDATE Perform gradient descent step on  $\mathcal{L}(\Theta) = (y_j - f_\Theta(\phi_j, a_j))^2$  with respect to  $\Theta$ 
28:  Every  $C$  steps reset the target action-value function  $\hat{f} = f$  by setting weights  $\hat{\Theta} = \Theta$ 
29: end for

```

implemented in `drl_algorithm.ipynb`. Both of these scripts are available at the root of the Github repository for this report (Batěk, 2024).

5.2.1. Simulating the Online Environment using KDD12

The KDD12 dataset was selected to simulate the online RL environment due to the fact that out of the three datasets introduced in section 4.2.1, it is the only dataset with clearly discernable user, context and advertisement features. Both Criteo and Avazu contain anonymized features, and it is therefore unclear what type of features these are.

All of the preprocessing steps discussed in section 4.2.1 including categorical value binning and encoding, numerical value normalization and target label weighting apply here as well, and these steps have therefore been encoded as in the preprocessing functions ϕ used for the model pretraining for the Offline Part, as well as the Online Algorithm. The pretraining of the DCN model f_Θ was conducted on first 157440 records the same training data as in chapter 4.

Our method for the online simulation proceeds as follows. A list of unique user ID u and query ID c entries from the KDD12 validation set has been compiled, ensuring that each u - c combination in this list had at least P observations in the validation set (where P is the chosen ad list length for the environment). For each session t in the simulation, we “observe” the user-query combination by selecting values from our pre-prepared list, thereby establishing the state s_t for the session. The set of available adverts \mathcal{A}_t is then retrieved by querying the KDD12 validation set for observations with the specific user-query entries that match the current state for the session. The DRL-AP algorithm then proceeds to construct ad list L_t by choosing P adverts from \mathcal{A}_t as described in algorithm 4. Finally the user feedback $\{r_h\}_{h=(t-1)P+1}^{tP}$ is then simply the target labels for the specific observations used to construct L_t .

5.2.2. Evaluation Metrics

We demonstrate the simulated performance of the DRL-AP algorithm in terms of **session level click through rate** and **regret**. The prior is simply defined as the number of ad observations chosen for L_t with positive click target labels, divided by list length P . For the latter, we adapt definition 3.1.6 as follows to suit the context of our simulation:

$$\mathcal{R}_T = \sum_{t=1}^K \left[\min(P, \sum_{r \in \mathcal{A}_t} r) - \sum_{r \in L_t} r \right]$$

The first term contained in the square brackets above represents the value for the optimal policy π^* . This policy should in theory be able to maximize the number of clicks for each session, given ad list \mathcal{A}_t and list length constraint P . The second term is simply equal to the value realized by the agent by constructing and displaying list L_t .

5.2.3. Hyperparameter Settings

The proof-of-concept simulation was run over a time horizon of 30 episodes, each containing 10 user-query sessions for Ad-list requests of length 10. The hyperparameter settings for the RL simulation have been chosen arbitrarily are stipulated in table 5.1.

Hyperparameter	Description	Value
N	Size of memory D	1800
K	Number of episodes	30
M	Sessions per episode	10
α	Explore parameter	1.0
P	Ad List length	6
ϵ	List-item level explore probability	0.5
γ	Future value discount	0.1

Table 5.1.: Hyperparameter settings for RL simulation

5.3. Deep CTR-RL Results and Discussion

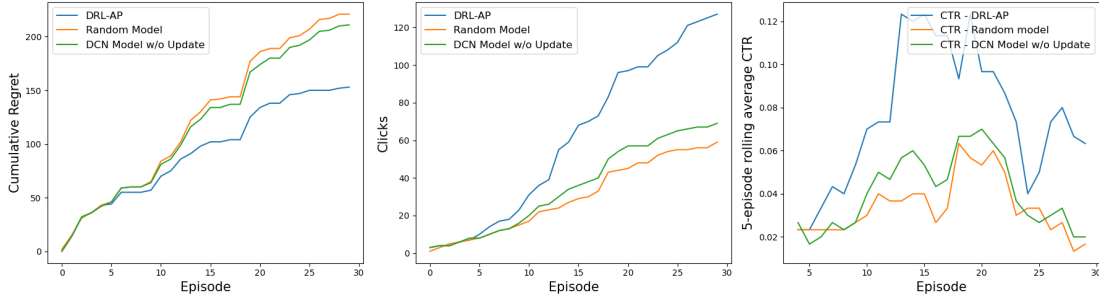


Figure 5.1.: Episode level Regret and CTR for DRL-AP and Random Model

Figure 4 shows the resulting episodic Cumulative Regret and 5-episode moving average Click Through rate for the simulation described in section 5.2.1. The results for the DRL-AP algorithm are shown in blue. As a benchmark, we simulated the results for a random model. In this case, the ads we chosen from \mathcal{A}_t uniformly at random. The mean result for the random model is represented by the orange line in both plots. Figure 5.1 clearly shows that the DRL-AP algorithm minimizes regret and therefore maximizes CTR better than the random model. This indicates that the predictive precision DCN model as a Q-function approximator significantly improves the Ad selection agents ability to choose adverts that the user will click on, which demonstrates the proof-of-concept for the DRL-AP algorithm.

T

6. Conclusion

Conclusion goes here.

A. Appendix

A.1. Abbreviations and Acronyms

Term	Definition	Reference
LR	Logistic Regression	2.3
FM	Factorization Machine	
FFM	Field-Aware Factorization Machine	
DNN	Deep Neural Network	
MLP	Multilayer Perceptron	

A.2. Notation

Symbol	Definition	Reference
\mathbf{x}	Feature vector, before pre-processing	
n	the number of features in \mathbf{x}	
x_i	The i -th feature in \mathbf{x}	
\mathbf{x}_i^{OH}	One-hot encoded vector representation of categorical feature i	
\mathbf{e}_i	Embedded vector representation of categorical feature i	
z_i	Mean and variance standardized value for feature i from \mathbf{x}	
$\tilde{\mathbf{x}}$	\mathbf{x} after categorical embedding and numerical standardization.	
f	Pre-sigmoid classification function	
Θ	Parameter vector for f	

A.3. Experiment Results

A.3.1. Experiment 1: Comparative Model Analysis

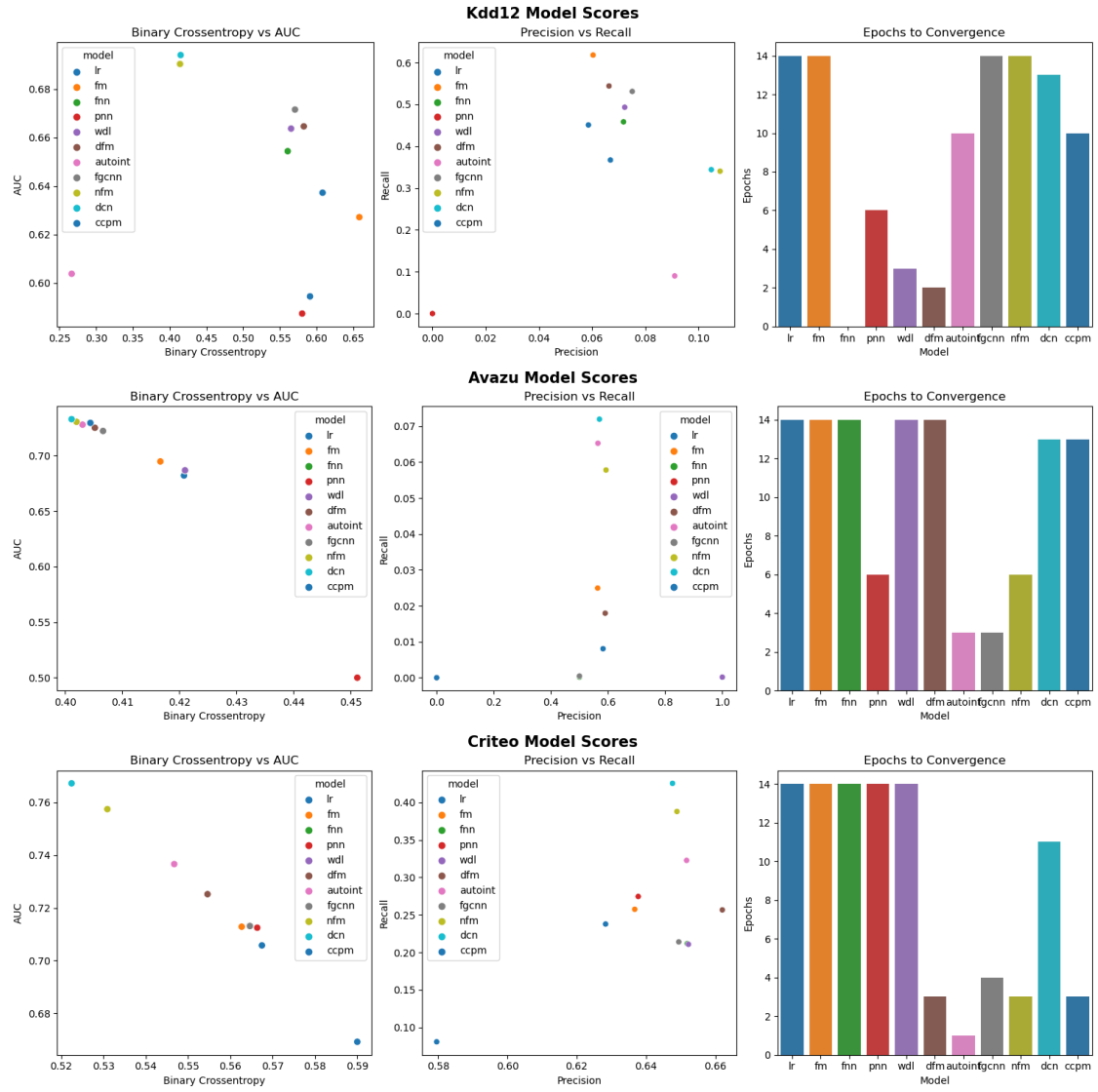


Figure A.1.: Experiment 1 Model Scores

Bibliography

- Yi Wang Aden. Kdd cup 2012, track 2, 2012. URL <https://kaggle.com/competitions/kddcup2012-track2>.
- Amazon Web Services. Amazon sagemaker data wrangler tool, 2024. URL <https://aws.amazon.com/sagemaker/data-wrangler/>.
- Peter Auer, Thomas Jaksch, and Ronald Ortner. Near-optimal regret bounds for reinforcement learning. In *Advances in Neural Information Processing Systems*. Curran Associates, Inc., 2008.
- Martin Batěk. Deep Reinforcement Learning for Ad Personalization, August 2024. URL <https://github.com/martinbatek/drl-ad-personalization>.
- Yin-Wen Chang, Cho-Jui Hsieh, Kai-Wei Chang, Michael Ringgaard, and Chih-Jen Lin. Training and testing low-degree polynomial data mappings via linear svm. *Journal of Machine Learning Research*, 11(4), 2010.
- Minmin Chen, Alex Beutel, Paul Covington, Sagar Jain, Francois Belletti, and Ed H. Chi. Top-k off-policy correction for a reinforce recommender system. In *Proceedings of the Twelfth ACM International Conference on Web Search and Data Mining*, WSDM '19, page 456–464, New York, NY, USA, 2019. Association for Computing Machinery. ISBN 9781450359405. doi: 10.1145/3289600.3290999. URL <https://doi.org/10.1145/3289600.3290999>.
- Chen Cheng, Fen Xia, Tong Zhang, Irwin King, and Michael R. Lyu. Gradient boosting factorization machines. In *Proceedings of the 8th ACM Conference on Recommender systems*, page 265–272, 2014.
- Heng-Tze Cheng, Levent Koc, Jeremiah Harmsen, Tal Shaked, Tushar Chandra, Hrishi Aradhye, Glen Anderson, Greg Corrado, Wei Chai, Mustafa Ispir, Rohan Anil, Zakaria Haque, Lichan Hong, Vihan Jain, Xiaobing Liu, and Hemal Shah. Wide & deep learning for recommender systems. In *Proceedings of the 1st Workshop on Deep Learning for Recommender Systems*, DLRS 2016, page 7–10, New York, NY, USA, 2016. Association for Computing Machinery. ISBN 9781450347952. doi: 10.1145/2988450.2988454. URL <https://doi.org/10.1145/2988450.2988454>.
- François Chollet et al. Keras. <https://github.com/keras-team/keras>, 2023.
- CXL. What is a “good” click-through rate? click-through rate benchmarks. URL <https://cxl.com/guides/click-through-rate/benchmarks/>.

G. Cybenko. Approximation by superpositions of a sigmoidal function. *Mathematics of control, signals, and systems*, 2(4):303–314, 1989. doi: 10.1007/BF02551274.

eMarketer. Digital advertising spending worldwide from 2021 to 2027 (in billion u.s. dollars). Technical report, Statista Inc., 2023. URL <https://www-statista-com.iclibezp1.cc.ic.ac.uk/statistics/237974/online-advertising-spending-worldwide-from-2021-to-2027>.

Thore Graepel, Joaquin Quinonero Candela, Thomas Borchert, and Ralf Herbrich. Web-scale bayesian click-through rate prediction for sponsored search advertising in microsoft’s bing search engine. Omnipress, 2010.

Liqiong Gu. Ad click-through rate prediction: A survey. In Christian S. Jensen, Ee-Peng Lim, De-Nian Yang, Chia-Hui Chang, Jianliang Xu, Wen-Chih Peng, Jen-Wei Huang, and Chih-Ya Shen, editors, *Database Systems for Advanced Applications. DASFAA 2021 International Workshops*, pages 140–153, Cham, 2021. Springer International Publishing. ISBN 978-3-030-73216-5.

Huifeng Guo, Ruiming Tang, Yunming Ye, Zhenguo Li, and Xiuqiang He. Deepfm: A factorization-machine based neural network for ctr prediction. *CoRR*, abs/1703.04247, 2017. URL <http://arxiv.org/abs/1703.04247>. 1703.04247.

John T. Hancock and Taghi M. Khoshgoftaar. Survey on categorical data for neural networks. *Journal of Big Data*, 7(1):28, 2020. doi: 10.1186/s40537-020-00305-w. URL <https://doi.org/10.1186/s40537-020-00305-w>. ID: Hancock2020.

Kaiming He, Xiangyu Zhang, Shaoqing Ren, and Jian Sun. Deep residual learning for image recognition. In *Proceedings of the IEEE conference on computer vision and pattern recognition*, page 770–778, 2016.

Xiangnan He and Tat-Seng Chua. Neural factorization machines for sparse predictive analytics, -08-16 2017.

Kurt Hornik, Maxwell Stinchcombe, and Halbert White. Multilayer feedforward networks are universal approximators. *Neural Networks*, 2(5):359–366, 1989. doi: 10.1016/0893-6080(89)90020-8. URL <https://www.sciencedirect.com/science/article/pii/0893608089900208>. ID: 271125.

Kurt Hornik, Maxwell Stinchcombe, and Halbert White. Universal approximation of an unknown mapping and its derivatives using multilayer feedforward networks. *Neural Networks*, 3(5):551–560, 1990. doi: 10.1016/0893-6080(90)90005-6.

Joseph G Ibrahim, Ming-Hui Chen, Debajyoti Sinha, JG Ibrahim, and MH Chen. *Bayesian survival analysis*, volume 2. Springer, 2001.

Sergey Ioffe. Batch normalization: Accelerating deep network training by reducing internal covariate shift. *arXiv preprint arXiv:1502.03167*, 2015.

- How Jing and Alexander J Smola. Neural survival recommender. In *Proceedings of the Tenth ACM International Conference on Web Search and Data Mining*, pages 515–524, 2017.
- Yuchin Juan, Yong Zhuang, Wei-Sheng Chin, and Chih-Jen Lin. Field-aware factorization machines for ctr prediction. In *10th ACM Conference on Recommender Systems*, RecSys '16, page 43–50, New York, NY, USA, 2016. Association for Computing Machinery. ISBN 9781450340359. doi: 10.1145/2959100.2959134. URL <https://doi.org/10.1145/2959100.2959134>.
- Diederik P. Kingma and Jimmy Ba. Adam: A method for stochastic optimization. *CoRR*, abs/1412.6980, 2014. URL <https://api.semanticscholar.org/CorpusID:6628106>.
- Alex Krizhevsky, Ilya Sutskever, and Geoffrey E. Hinton. Imagenet classification with deep convolutional neural networks. *Communications of the ACM*, 60(6):84–90, 2017.
- Yann LeCun, Léon Bottou, Yoshua Bengio, and Patrick Haffner. Gradient-based learning applied to document recognition. *Proceedings of the IEEE*, 86(11):2278–2324, 1998.
- Liu, Yu, Wu, and Wang. A convolutional click prediction model, -10-17 2015.
- Bin Liu, Ruiming Tang, Yingzhi Chen, Jinkai Yu, Huifeng Guo, and Yuzhou Zhang. Feature generation by convolutional neural network for click-through rate prediction. In *The World Wide Web Conference*, page 1119–1129, 2019.
- Meta AI Research. Papers with code, 2024. URL <https://paperswithcode.com/>.
- Volodymyr Mnih, Koray Kavukcuoglu, David Silver, Andrei A. Rusu, Joel Veness, Marc G. Bellemare, Alex Graves, Martin Riedmiller, Andreas K. Fidjeland, Georg Ostrovski, Stig Petersen, Charles Beattie, Amir Sadik, Ioannis Antonoglou, Helen King, Dharmashan Kumaran, Daan Wierstra, Shane Legg, and Demis Hassabis. Human-level control through deep reinforcement learning. *Nature*, 518(7540):529–533, February 26 2015. doi: 10.1038/nature14236. LR: 20220408; JID: 0410462; CIN: Nature. 2015 Feb 26;518(7540):486-7. doi: 10.1038/518486a. PMID: 25719660; 2014/07/10 00:00 [received]; 2015/01/16 00:00 [accepted]; 2015/02/27 06:00 [entrez]; 2015/02/27 06:00 [pubmed]; 2015/04/16 06:00 [medline]; AID: nature14236 [pii]; ppublish.
- Ciara Pike-Burke. Optimism/thompson sampling, 2024a.
- Ciara Pike-Burke. Learning agents mlds course, 2024b.
- Martin L Puterman. *Markov decision processes: discrete stochastic dynamic programming*. John Wiley & Sons, 2014.
- Yanru Qu, Han Chai, Kan Ren, Weinan Zhang, Yong Yu, Ying Wen, and Jun Wang. Product-based neural networks for user response prediction. In *2016 IEEE 16th International Conference on Data Mining (ICDM)*, pages 1149–1154. IEEE, 2016. ISBN 2374-8486. doi: 10.1109/ICDM.2016.0151. ID: 1.

- Yanru Qu, Bohui Fang, Weinan Zhang, Ruiming Tang, Minzhe Niu, Huifeng Guo, Yong Yu, and Xiuqiang He. Product-based neural networks for user response prediction over multi-field categorical data. *ACM Trans.Inf.Syst.*, 37(1), oct 2018. doi: 10.1145/3233770. URL <https://doi.org/10.1145/3233770>.
- Steffen Rendle. Factorization machines. In *2010 IEEE International Conference on Data Mining*, pages 995–1000, 2010. ISBN 1550-4786. doi: 10.1109/ICDM.2010.127. ID: 1.
- Matthew Richardson, Ewa Dominowska, and Robert Ragno. Predicting clicks: Estimating the click-through rate for new ads. In *International Conference on World Wide Web*, WWW '07, page 521–530, New York, NY, USA, 2007. Association for Computing Machinery. doi: 10.1145/1242572.1242643. URL <https://doi.org/10.1145/1242572.1242643>.
- Herbert Robbins and Sutton Monro. A stochastic approximation method. *The annals of mathematical statistics*, pages 400–407, 1951.
- Shai Shalev-Shwartz, Ohad Shamir, and Shaked Shammah. Failures of gradient-based deep learning. In Doina Precup and Yee Whye Teh, editors, *Proceedings of the 34th International Conference on Machine Learning*, volume 70 of *Proceedings of Machine Learning Research*, page 3067–3075. PMLR, aug 2017. URL <https://proceedings.mlr.press/v70/shalev-shwartz17a.html>.
- Weichen Shen. Deepctr: Easy-to-use, modular and extendible package of deep-learning based ctr models, 2017. URL <https://github.com/shenweichen/deepctr>.
- Song, Shi, Xiao, Duan, Xu, Zhang, and Tang. AutoInt, -11-03 2019.
- Nitish Srivastava, Geoffrey Hinton, Alex Krizhevsky, Ilya Sutskever, and Ruslan Salakhutdinov. Dropout: a simple way to prevent neural networks from overfitting. *The journal of machine learning research*, 15(1):1929–1958, 2014.
- Jean-Baptiste Tien, joycenv, and Olivier Chapelle. Display advertising challenge, 2014. URL <https://kaggle.com/competitions/criteo-display-ad-challenge>.
- Hado van Hasselt, Arthur Guez, and David Silver. Deep reinforcement learning with double q-learning. *Proceedings of the AAAI Conference on Artificial Intelligence*, 30(1), March 2016. doi: 10.1609/aaai.v30i1.10295. URL <https://ojs.aaai.org/index.php/AAAI/article/view/10295>.
- Ruoxi Wang, Bin Fu, Gang Fu, and Mingliang Wang. Deep & cross network for ad click predictions. In *Proceedings of the ADKDD'17*, ADKDD'17, New York, NY, USA, 2017. Association for Computing Machinery. ISBN 9781450351942. doi: 10.1145/3124749.3124754. URL <https://doi.org/10.1145/3124749.3124754>.
- Steve Wang and Will Cukierski. Click-through rate prediction, 2014. URL <https://kaggle.com/competitions/avazu-ctr-prediction>.

- Xu Wang, Sen Wang, Xingxing Liang, Dawei Zhao, Jincai Huang, Xin Xu, Bin Dai, and Qiguang Miao. Deep reinforcement learning: A survey. *IEEE Transactions on Neural Networks and Learning Systems*, 35(4):5064–5078, 2024. doi: 10.1109/TNNLS.2022.3207346.
- Christopher John Cornish Hellaby Watkins. *Learning from delayed rewards*. PhD thesis, 1989.
- Kevin Webster. Week 2: Multilayer perceptron, 2024.
- Jun Xiao, Hao Ye, Xiangnan He, Hanwang Zhang, Fei Wu, and Tat-Seng Chua. Attentional factorization machines: Learning the weight of feature interactions via attention networks *, 2017. URL <https://arxiv.org/abs/1708.04617>.
- Pengtao Zhang and Junlin Zhang. Memonet: Memorizing all cross features’ representations efficiently via multi-hash codebook network for ctr prediction, -10-21 2023.
- Weinan Zhang, Tianming Du, and Jun Wang. Deep learning over multi-field categorical data: A case study on user response prediction, 2016. URL <https://arxiv.org/abs/1601.02376>. 1601.02376.
- Weinan Zhang, Jiarui Qin, Wei Guo, Ruiming Tang, and Xiuqiang He. Deep learning for click-through rate estimation, 21 Apr 2021. URL <https://arxiv.org/abs/2104.10584>.
- Guanjie Zheng, Fuzheng Zhang, Zihan Zheng, Yang Xiang, Nicholas Jing Yuan, Xing Xie, and Zhenhui Li. Drn: A deep reinforcement learning framework for news recommendation. In *2018 World Wide Web Conference*, pages 167–176, Lyon, France, 2018. International World Wide Web Conferences Steering Committee. doi: 10.1145/3178876.3185994. URL <https://doi.org/10.1145/3178876.3185994>.